

Contact Binary Stars in Survey Data

A *thesis submitted in partial fulfillment of the requirements of a degree of Bachelor of Arts in Physics at Pomona College*



Franklin Marsh
with advisor
Philip I. Choi, Ph.D.
Professor of Astronomy
Pomona College

August 15, 2016

Abstract

Acknowledgments

To Mom and Dad

Contents

1	Introduction - Contact Binaries at the Intersection	6
2	The Contact Binary Star	8
2.1	<i>Discovery</i>	8
2.2	Physical Characteristics	11
2.2.1	The Main-Sequence Star	12
2.2.2	The Roche Potential	14
2.2.3	The Geometrical Elements of Contact Binary Systems	17
2.2.4	The Criterion for Stellar Convection	19
2.2.5	Thermal Equilibrium Models	20
2.3	Interior Structure	21
2.3.1	Common-Envelope Evolution	22
2.4	Frequency and Density	23
2.5	Mechanisms of Formation	23
2.6	Evolution in the Contact State	24
2.7	Evolution out of the Contact State	24
2.8	Early-Type Contact Binaries	26
2.9	Magnetic Activity	27
2.10	Remaining Questions	29
3	Observations	29
3.1	Images of Contact Binaries	29
3.2	Photometry of Contact Binaries	31
3.2.1	Amplitude	33
3.2.2	Difference Between Eclipse Minima	33
3.2.3	Difference Between Out-of-Eclipse Maxima	33
3.2.4	Eclipse Width at Half-Minimum	33
3.3	Spectra of Contact Binaries	33
3.4	X-ray and Ultraviolet Data on Contact Binaries	33
3.5	The Kepler Spacecraft	34
3.6	The Sloan Digital Sky Survey	34
3.7	The SuperWASP Survey	34
3.8	The LINEAR Survey	35
3.9	The Catalina Surveys	35
3.10	Other Surveys	35

3.11 Future Surveys	35
4 Analysis Techniques	36
4.1 Physical Light-Curve Modeling	36
4.2 O-C Analysis	36
4.3 Doppler Imaging	38
5 Pause	38
6 Light-curve Morphology	40
6.1 Our Observations	41
6.2 Light-curve Features	41
7 Luminosity Variation on a Decadal Timescale	45
8 Detection of Flares	45
9 Conclusion	47

1 Introduction - Contact Binaries at the Intersection

Q: Why are contact binaries interesting (and important!)?

The contact binary star is placed at the intersection of some of the largest questions in modern astronomy.

Modern observational techniques have allowed for the detection of transients (light sources that appear for a brief time and then disappear) in vast quantities. The supernova is a common example of a transient. By observing hundreds of supernovae, astronomers discovered that not all supernovae are the same - some are brighter than others, some last longer than others. They have also discovered transients that are not supernovae. In recent years, astronomers have been gaining information about transients that are much brighter than novae, but dimmer than supernovae. They named this class “Intermediate Luminosity Red Transients”. Until recently, there was not a viable physical model for these transients. In late 2008, an ILRT emerged in the constellation of scorpius. When astronomers looked in archival data - they found a contact binary in the spot where the nova had occurred. The leading theory is that the merger of a contact binary system causes these Intermediate Luminosity Red Transients.

While contact binaries systems are very different than the sun, they are important tools for testing the solar-stellar connection: the idea that the sun is similar to other stars and that we can learn about other stars by observing the sun. While the sun takes almost a month to rotate, almost all contact binaries complete a full orbit in less than a day. Contact binaries have much greater angular momenta than single stars of the same spectral type. Contact binaries have strong magnetic fields (as much as 1000 times stronger than the sun’s), because they are moving about their rotational axis much more quickly. We will see that each component of a solar type contact binary exhibits a similar structure to the sun: a radiative inner layer surrounded by a convective envelope. For this reason, contact binaries exhibit the same magnetic phenomena (such as starspots, and flares) as the sun does - except these phenomena on contact binaries are much more dramatic, owing to the stronger magnetic field strength. The dramatic magnetic phenomena in contact binaries is observable from large distances. From the earth, we can monitor the magnetic activity of thousands of contact binary stars. This is the subject of much of the original work in this thesis.

habitability - could planets exist around such systems? Would massive flares and orbital instabilities render life impossible?

With the recent direct observation of gravitational waves by LIGO, there has been renewed interest in gravitational wave sources. It was found that the source of the first gravitational wave detection was two intermediate mass ($20 - 30M_{\odot}$) black holes, which was an unexpected result.

Massive and short-lived-contact binary stars offer a solution to this problem.
gravitational waves - massive contact binaries consisting of O and B Type main sequence stars.

As we will learn, contact binaries are a well-defined class with strict relationships between parameters like mass, luminosity, temperature, and orbital period. This means that by measuring a few parameters, many others can be accurately predicted. There are theoretically and empirically defined relationships between a contact binary's period, temperature, and luminosity. This means, by measuring a contact binary's orbital period (which can be done easily and precisely) astronomers can predict the contact binary's absolute luminosity (which is difficult to measure with traditional methods). For this reason, contact binaries are important *standard candles*. Contact binaries are much more common than Cepheid Variables, or RR Lyrae variables. They can be used to trace the structure of the milky way galaxy, and accurately determine distances to other galaxies.

The observed frequency and spatial density of contact binary systems can provide important information about the density of young star forming regions.

In these ways, the contact binary stands at the intersection of time-domain, solar, gravitational wave, and stellar astronomy. But contact binaries also stand at another important intersection: the intersection of “old” and “new” observational techniques.

We roughly can split observational astronomy into two modes, which I will call:

1. Survey Mode: Look out and see what there is to see.
2. Target Mode: Observe very specific set of objects in a way tailored to learn about known phenomena.

As we will see, the first contact binary was discovered in a survey.

In the 20th century, the science of astronomy was “data poor”. The limiting factor of discovery was observations from large telescopes of the day. The possession of astronomical data enabled the science. If a scientist had new, proprietary data, science would come out of it.

At the turn of the 21st century (enabled by advances in data storage, processing and robotics, and as a direct result of Moore’s law) observational astronomical science began to shift modes.

Old telescopes were being remodeled, old gears, motors and lenses were being replaced with robotic systems, enabling their autonomous operation. New telescopes were being constructed with the express purpose of deeply surveying the sky - with minimal human intervention. No longer inhibited by human operators, telescopes could image the sky continuously - dawn to dusk. Data poured from these telescopes like water from a firehose. The new images filled massive stacks of servers: for the first time, astronomers were “data rich”.

The monstrous stream of data had to be filtered. Scientists interested in new discoveries

had to find the proverbial needle in the haystack. The most productive scientist was no longer the scientist with access to the best data, it became the scientist with the best techniques for filtering, stacking, folding, combining, or otherwise analyzing the data. Astronomers started shifting back to “Survey Mode”.

Asteroids were discovered by the thousands. The rate of supernova discovery accelerated from one every few years to *one every night*. The number of known eclipsing binaries ballooned from just over a thousand, to tens of thousands. The number of galaxies with known distances lept from BLANK to BLANK. This progress is accelerating: within the decade, at least three major sky surveys of unprecedented depth and cadence will come online.

In the 21st century, we can study thousands of contact binary systems at once, using data from all-sky surveys. This approach presents huge advantages over painstakingly observing single contact binary systems. However, there are also weaknesses.

Many of the techniques that have been developed for extracting science out of observational data do not work well in survey data. We are forced to develop new techniques

present tense

In §2 I provide a brief history of the discovery of the first contact binary star, and outline major leaps of understanding in the field. In §3, I discuss the types of observations that can be used to learn about contact systems. In §4, I explain the ways that astronomers are able to use measurements to physically characterize contact systems.

I then present original research that I have undertaken with Dr. Tom Prince, Dr. Ashish Mahabal, Dr. Eric Bellm, and Dr. Andrew Drake at the California Institute of Technology. In §6, we discuss how light-curve characteristics vary as a function of temperature. In §7, we present the results of the search for variability in contact binary luminosity on decadal time scales. In §8, we present the results of a search for flares on contact binary stars in survey data. Each section is prefaced with a list of driving questions (*Q:*), which are questions that the reader will find answered in that section.

What I hope this thesis is: 1. An introduction to the field of 2. People have developed techniques for studying the sky when astronomy was data-poor: how can we adapt these techniques to be useful in data-rich astronomy. 3. A roadmap for a promising summer student to use when continuing this work, either at Caltech or Pomona.

2 The Contact Binary Star

2.1 Discovery

Q: How was the first contact binary star discovered?

To understand the history of the study of contact binaries, we must start at the source:

the advent of a precise way of measuring the brightness of a celestial object.

In 1861, J.K.F. Zöllner, developed the first practical photometer. In Zöllner's photometer , the image of a real star as focused by a 5" objective lens was compared with the light of an artificial star, produced by a bunsen-like gas burner, in the same field of view [Stauber-mann, 2000]. The brightness of this artificial star could be adjusted by changing the relative orientation of two prisms, until it matched that of the real star. By recording the relative angle of the prisms when the brightness of the artificial and real star were equal, a photo-metric measurement could be obtained. In the 1860s, Zöllner supplied 22 photometers to the great observatories throughout the western world. One of these photometers arrived at the Potsdam Observatory , 15 miles southwest of Berlin's city center [Krisciunas, 2001].

Karl Hermann Gustav Müller , and Paul Friedrich Ferdinand Kempf collaborated on ob-servations for the Potsdam *Photometrische Durchmusterung des Nördlichen Himmels* (Photometric Catalogue of the Northern Heavens), one of the three great photometric catalogues of the late nineteenth century [Bolt et al., 2007]. When it was finished, it contained the brightnesses and colors of roughly 14,000 stars down to visual magnitude 7.5 - a monumen-tal undertaking.

While Kempf and Müller were making the initial observations for Part III of their *Durch-musterung*, they discovered that two measurements of an otherwise inconspicuous star (the first made in 1899, the second made in 1901) differed by an amount that was greater than was expected. In their survey, each star that showed the potential for variability was observed at a later date to verify the nature of variability.

At the Potsdam Observatory on January 14th, 1903, the sun set at 4:20pm. An hour and a half later, (at 5:56pm) Kempf and Müller began constructing a complete light-curve of *BD + 56°.1400*, which would later be named W Ursae Majoris. They observed until 10:30PM. Follow-up observations three nights later allowed for the construction of the first light-curve of a contact binary star (Figure 2).



Figure 1: Fig. 4 from Staubermann [2000], showing a modern reproduction of a Zöllner photometer. Note the tube: the refractor telescope.

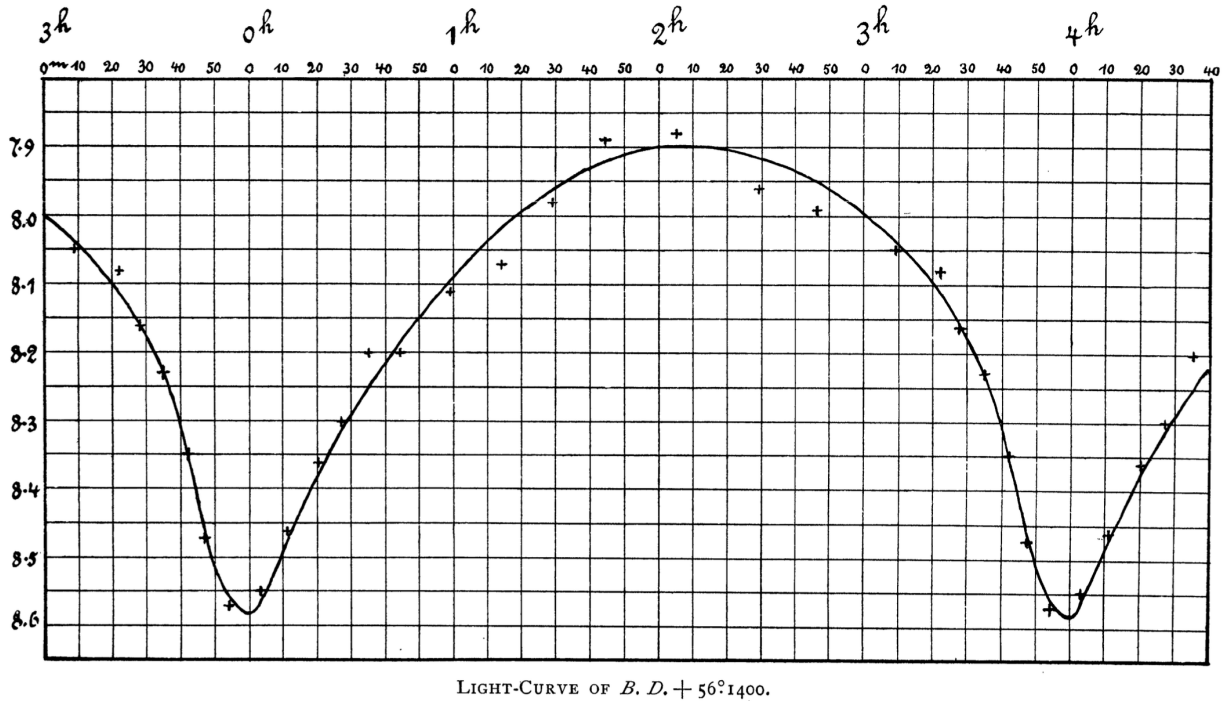


Figure 2: The first light-curve of a contact binary star. Note that the solid curve is interpolated by eye and drawn carefully in pen. Figure 1 from Müller and Kempf [1903].

The shape of the light-curve was unlike anything that Müller and Kempf had seen before, and they struggle to think of a physical system that can produce such a light curve, rejecting many hypotheses (LIST EXISTING HYPOTHESES), before speculating:

“We may finally consider the hypothesis that the light-variation is produced by two celestial bodies almost equal in size and luminosity whose surfaces are at a slight distance from each other, and which at times almost centrally occult each other in their revolution... On this hypothesis we have only one difficulty, and the not inconsiderable one, as to whether such a system is mechanically possible and can remain stable for any length of time.”

This is the beginning. In this thesis, written 114 years the initial discovery, we will journey to the forefront of contact binary research.

2.2 Physical Characteristics

Q: What are contact binaries made of? How do contact binaries generate their luminosity? Why are contact binaries shaped like peanuts? How are eclipsing binaries classified? How common are contact binaries compared to all main-sequence stars? How do contact binaries form? How do contact binaries evolve over their lifetime? What is the ultimate fate of a contact binary? What do we know about the most massive contact binaries? What are some interesting magnetic phenomena that occur on contact binaries?

In this section, we will work to gain a physical understanding of contact binary systems.

Contact binary stars are made up of two main-sequence stars. In §2.2.1 we will understand what main-sequence stars are like on the inside, how energy is generated in the cores of main-sequence stars, and how this energy is transported to the surface.

Once we have got a firm grasp of the properties of main-sequence stars, we will bring two of them together to form a contact binary. In §2.2.2, we learn that we must change the potential that the stellar matter exists in from the point potential to the Roche potential. Also, the components of contact binary stars can transfer mass and energy, from one to the other. We must take this into account when building our model.

In §??, we will learn how common contact binary stars as compared to single main-sequence stars. We will also learn how common they are in the Milky Way galaxy.

In §??, we will learn how contact binaries are formed. We will be introduced to the concepts of angular momentum loss (AML), and Kozai-Lidov cycles.

In §??, we will learn how contact binaries evolve during their lifetimes. We will see how this evolution can drive changes in the observable properties of contact binary systems.

[p.76, Webbink, 2003] excellent review of remaining problems in contact binary study.

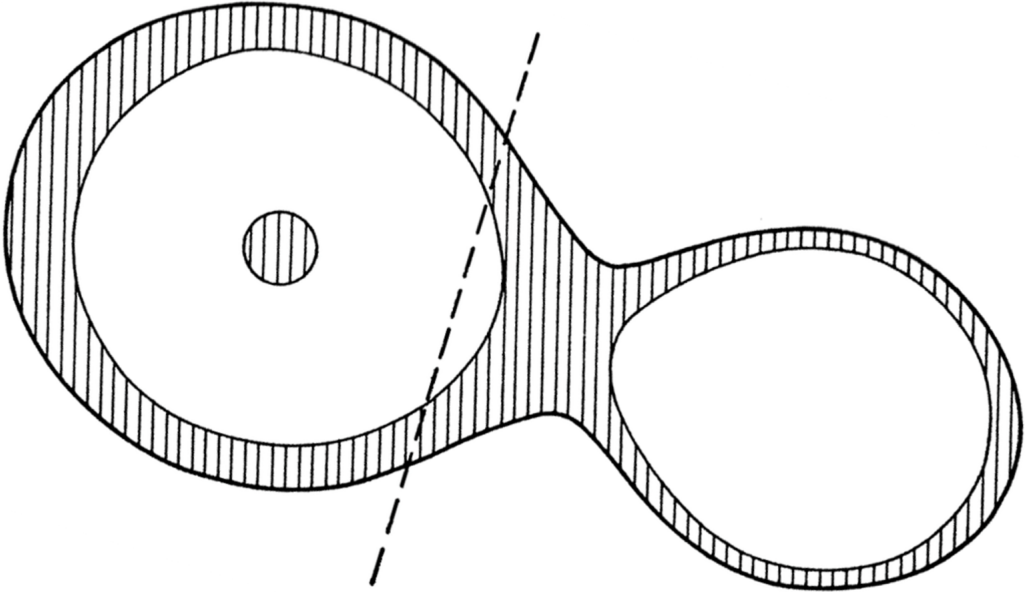
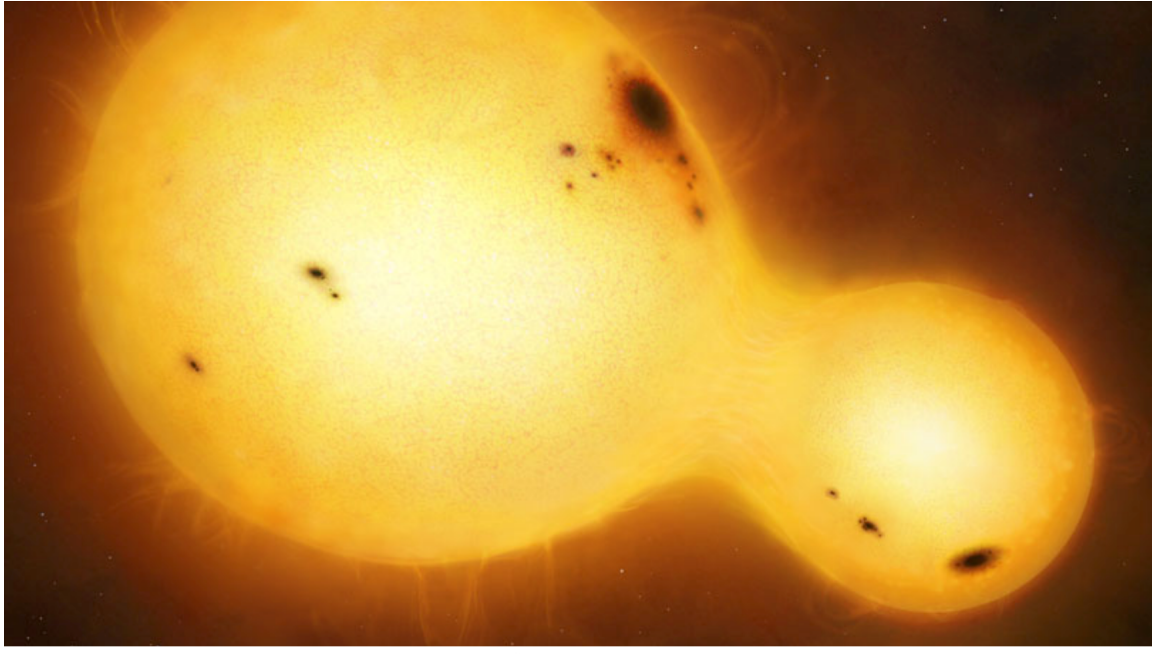


Figure 3: Model for a contact binary system. The hatched areas denote convection zones, and the vertical dashed line is the axis of rotation. Figure 1 from Lucy [1968a].

2.2.1 The Main-Sequence Star

In order to understand the internal structure of contact binaries, we must first understand the structure of their two components: main-sequence stars. The main sequence was an empirically derived group: When astronomers started recording the luminosity and color of lots of stars, they observed that most stars obeyed a relationship between luminosity

and color. This relationship can be visualized in an *Hertzsprung-Russell Diagram* (or H-R Diagram), like Figure 4. They called the main cluster of points on this diagram the “Main Sequence”. The most familiar example of a main sequence star is our Sun. When a star is fusing hydrogen into helium at its core, we say that it is on the main sequence.

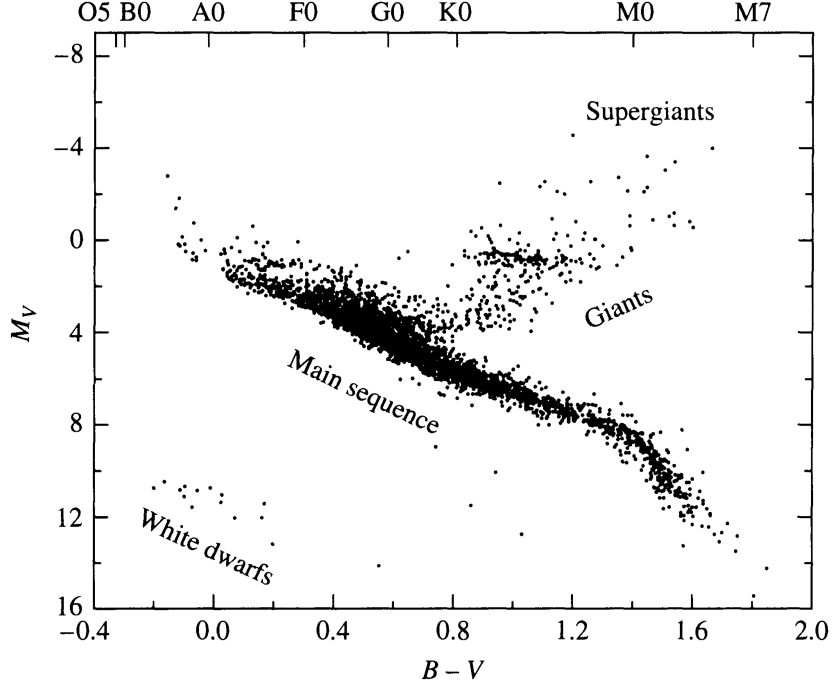


Figure 4: An observer’s Hertsprung-Russel (H-R) diagram. The data are from the Hipparcos catalog. Figure 8.13 from Carroll and Ostlie [2006].

Astronomers have an excellent understanding of the observables (like mass, luminosity, or temperature) of main-sequence stars. Models of main-sequence stars that rely on basic time-independent equations of stellar structure have been successful.

The time-independent equations of stellar structure are a set of relationships between the properties of main sequence stars. They tell how pressure (P), enclosed mass (M_r), enclosed luminosity (L_r), and temperature (T) change as a function of radius r . You will notice that that all of the following equations are actually derivatives. When we supply the appropriate boundary condition (eg. “the temperature T at 1 solar radius is 5800K”), the equations allow for the complete solution of the run of temperature, pressure, and mass through the star.

$$\frac{dP}{dr} = -G \frac{M_r \rho}{r^2} \quad (2.1)$$

$$\frac{dM_r}{dr} = 4\pi r^2 \rho \quad (2.2)$$

$$\frac{dL_r}{dr} = 4\pi r^2 \rho \epsilon \quad (2.3)$$

$$\frac{dT}{dr} = -\frac{3}{4ac} \frac{\bar{\kappa} \rho}{T^3} \frac{L_r}{4\pi r^2} \quad (2.4)$$

2.2.2 The Roche Potential

In the equations of stellar structure, there is a hidden assumption. These time-independent equations of stellar structure assume that the stellar matter exists in the potential of a point mass:

$$\Psi_{\text{point}} = \frac{GM}{r} \quad (2.5)$$

However, a contact binary system cannot be modeled as a point mass. A contact binary most definitely contains *two* masses, because it contains two stellar components. We can approximate these stellar components as two point masses, separated by a distance a .

In contact binary systems, the two stellar components are rapidly rotating about their center of mass.

The Roche model assumes: synchronous rotation, circular orbits, two point masses, in the rotating frame [Kopal, 1959] :

Mochnacki [1984]:

“In Cartesian coordinates, with the origin at the center of mass of the primary, the x -axis aligned with the centers of mass, and the z -axis parallel to the rotation axis, the potential at a point (x,y,z) co-rotating with binary system is given by: ”

$$\Psi_{\text{roche}}(x, y, z) = -\frac{G(M_1 + M_2)}{2a} C \quad (2.6)$$

where

$$C(x, y, z) = \frac{2}{1+q} \frac{1}{(x^2 + y^2 + z^2)^{\frac{1}{2}}} + \frac{2q}{1+q} \frac{1}{1+q[[(x-1)^2 + y^2 + z^2]^{\frac{1}{2}}]} + (x - \frac{q}{1+q})^2 + y^2 \quad (2.7)$$

$q = \frac{m_2}{m_1}$, (x, y, z) are in units of a , the separation between the two point masses.

The Roche potential has points where $\nabla \Psi = 0$, called Lagrange Points (see Figure ??).

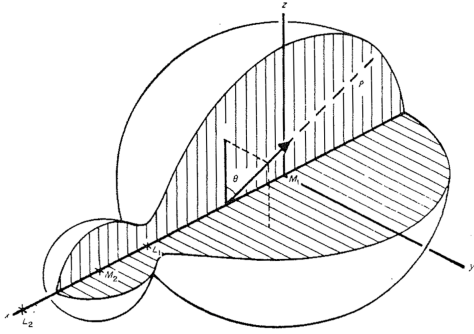


Figure 5: The coordinate system used in equations 2.6 and 2.7 to describe the potential Ψ of a contact binary system. Figure 1 from Mochnacki and Doughty [1972]

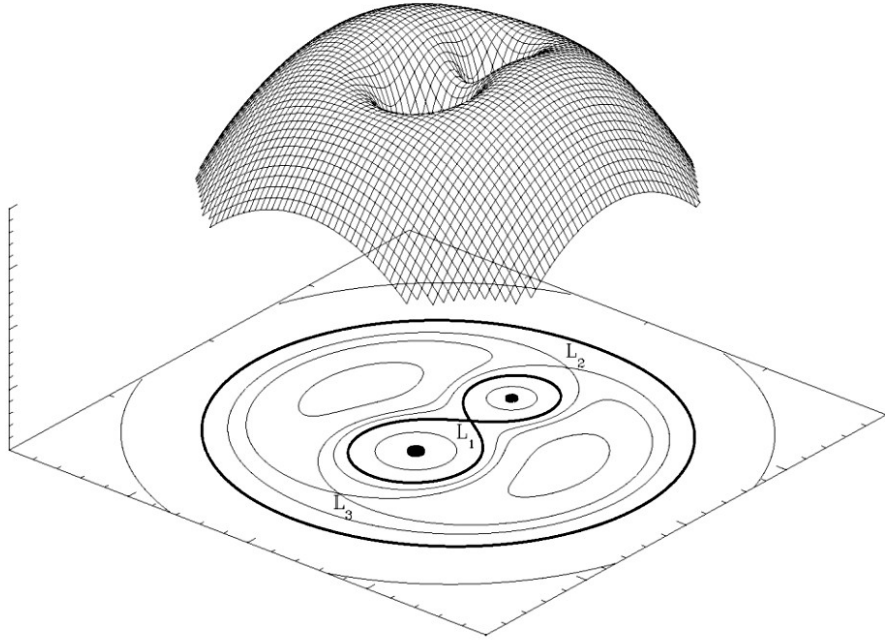


Figure 6: A composite 3D and contour plot of the Roche potential. The Roche lobe is the dark equipotential curve shaped like the ∞ symbol. Three out of the five Lagrange points are labelled L_1, L_2, L_3 . [Sluys, 2006]

Now that we understand the shape of the Roche potential, we can learn how the Roche potential is used to classify eclipsing binary stars, in a scheme primarily developed by the work of Kopal [1959].

In this scheme, eclipsing binaries are classified according to the location of the two photospheres relative to certain Roche equipotentials. In Figure 7, we see three types of eclipsing binaries. In Detached systems, the photosphere of each component is well within the Roche

lobe (the equipotential curve shaped like ∞). In a Semi-detached configuration, the photosphere of one component completely fills its Roche lobe (touching the L_1 point, while the photosphere of the other component remains well within its Roche lobe. In Overcontact systems, both components *overfill* the Roche lobe, and a bridge of stellar material connects the two components, covering the L_1 point [Terrell, 2001].

Now we know how Detached, Semi-Detached, and Overcontact binaries are classified - but wait: Where are the *Contact Binaries*? In this section, we have been referring to contact binaries as “Overcontact Binaries”. But why did we have to make the name change?

Since the first half of the 20th century, most astronomers believe that the term “contact” means that the photospheres of the two components are touching physically. This is incorrect, according to the original classification scheme of Kopal [1959]. He intended contact to mean that the photospheres of the stars were in contact with their Roche Lobes, (the inner Jacobi Equipotential). Though the term ”contact” binary is technically incorrect, it is the most common usage in the literature, and is now the accepted name for these kinds of stars. For an excellent review of this naming issue, see Wilson [2001]

The Roche lobe, (as we have been calling it) is also referred to as the *Inner Jacobi Equipotential*. There also exists an *Outer Jacobi Equipotential*. In Figure 7, the Outer Jacobi Equipotential is the outer-most curve that is drawn. It passes through the L_2 point.

An important note on the semantics of binary star classification. Kuiper [1941]

For an excellent review, see: [Kallrath and Milone, 2009]

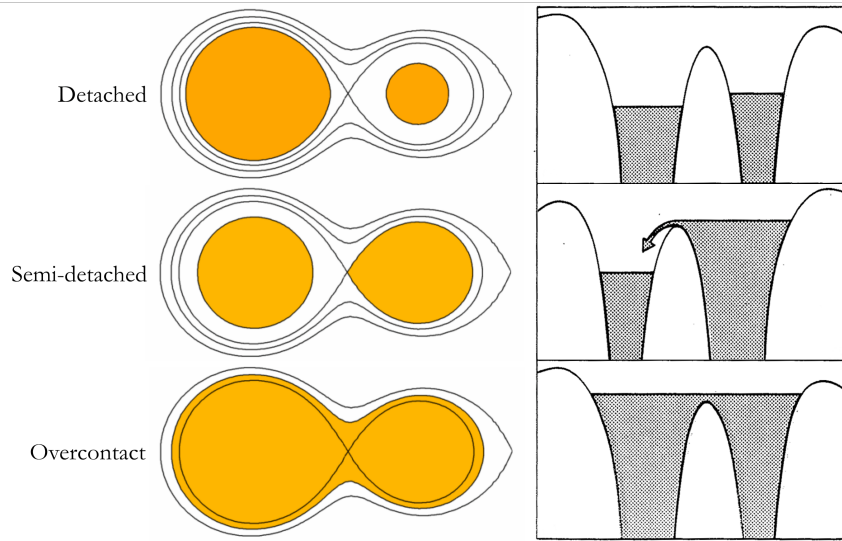


Figure 7: Types of eclipsing binary systems based on Roche geometry. In the bottom panel, (labelled “overcontact”), the photosphere of the star (shaded in orange), lies between the inner and outer Jacobi equipotentials. Figures 2,3, and 4 from Terrell [2001], and Figure 1.4 from Pringle and Wade [1985]

2.2.3 The Geometrical Elements of Contact Binary Systems

In the previous section, we have learned how to differentiate contact binary systems from the other types of eclipsing binary stars. In this section, we will learn how to describe specific contact binaries in terms of their geometrical elements. When we refer to the geometry of the contact binary system, we are really referring to the geometry of its photosphere. The vast majority of what we know of contact binary systems comes from their visible light-curves, which is why there is the convention of treating the photosphere as the “boundary” of the system.

Astronomers have developed a set of geometrical elements that can describe the location of the photosphere with respect to certain Roche equipotentials .

The first geometrical element of note is the mass ratio $q = \frac{M_1}{M_2}$ of the contact binary. The mass ratio is an important geometrical element in that it influences the shape of the Roche potential. We can see the effect of the mass-ratio term in equation 2.7. The Roche potential for a system with a mass ratio of unity (one) is perfectly symmetrical about the L_1 point. The Roche potential for a system with a mass ratio that is far from unity is not symmetrical about the L_1 point: the more massive component has an inner Jacobi equipotential that encloses more area.

The second geometrical element is the Roche lobe fill-out factor, f . This is the element that is used to describe the location of the photosphere with respect to the inner and outer Jacobi equipotentials.

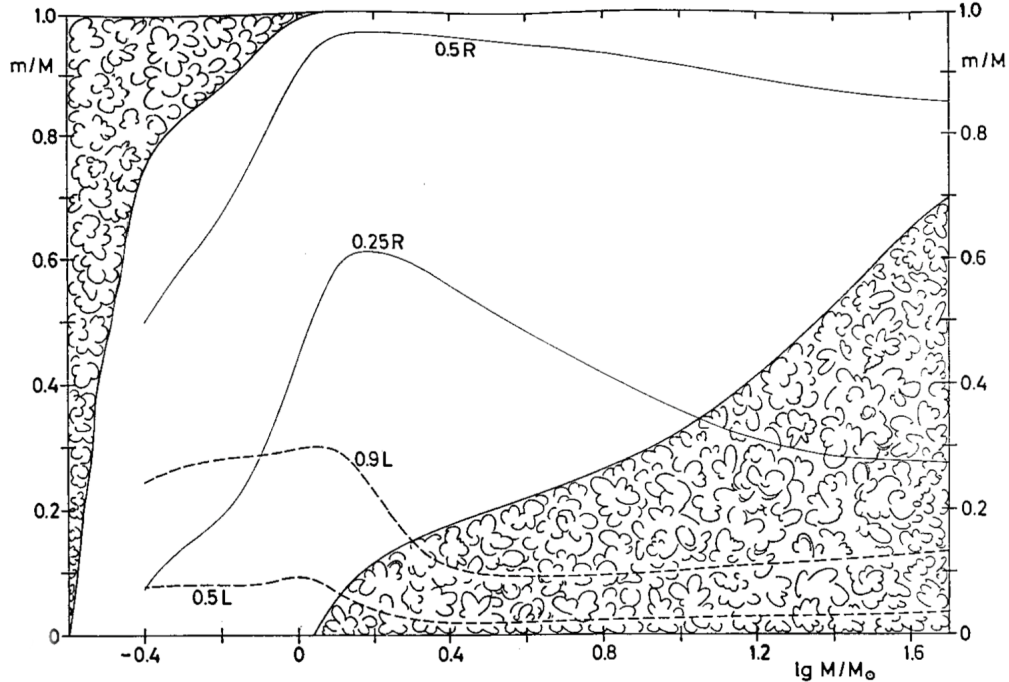


Figure 8: The mass values m from centre to surface are plotted against the stellar mass M for zero-age main-sequence models. ‘‘Cloudy’’ areas indicate the extent of the convective zones inside the models. Two solid lines give the m values at which r is $1/4$ and $1/2$ of the total radius R . The dashed lines show the mass elements inside which 50% and 90% of the total luminosity L are produced. Figure 22.7 from (pp. 212) of Kippenhahn et al. [1990].

Energy is generated at the core of low mass main sequence stars via the Proton-Proton Chain, or *pp chain*. The pp chain has three branches, each producing helium out of Hydrogen (H), Helium (He) and Beryllium (Be).

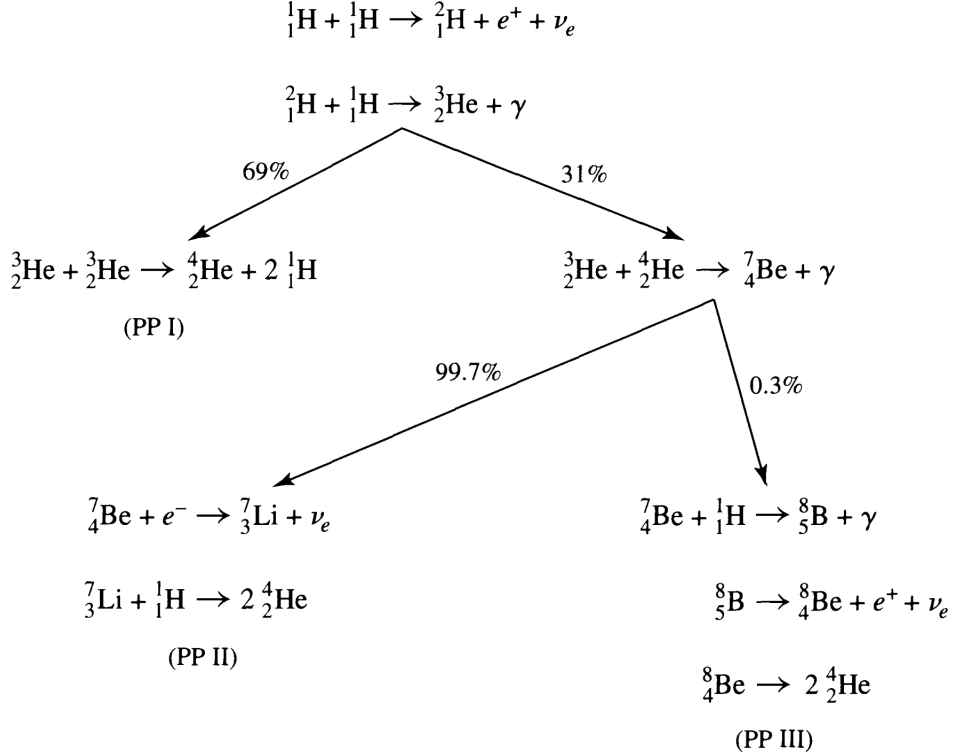


Figure 9: A diagram of pp chain reactions. Percentages by the arrows indicate the branching ratios, revealing that the PP I and PP II chains occur much more frequently than the PP III chain. Figure 10.8 from Carroll and Ostlie [2006].

The energy produced by all three branches of the pp chain can be represented:

$$\epsilon_{pp} = 0.241 \rho X^2 f_{pp} \psi_{pp} C_{pp} T_6^{-2/3} e^{-33.80 T_6^{-1/3}} \text{ W kg}^{-1} \quad (2.8)$$

Where $T_6 \equiv T/10^6$ K. When we expand Equation 2.8 in a power law about the solar core temperature of $T_{\odot, \text{core}} = 1.5 \times 10^7$ K, we see that the resulting power law has a T^4 dependence near $T_{\odot, \text{core}}$:

$$\epsilon_{pp} \approx \epsilon'_{0,pp} \rho X^2 f_{pp} \psi_{pp} C_{pp} T_6^4 \quad (2.9)$$

2.2.4 The Criterion for Stellar Convection

In our study of contact binary stars, we will find it useful to derive the conditions necessary for stellar convection to occur. We follow closely the analysis presented in Carroll and Ostlie [2006].

The two primary methods of energy transport in main-sequence stars are convection, and radiation. In radiation, the stellar material is in hydrostatic equilibrium, and energy

is transported through it via electromagnetic waves. If conditions are such that radiation cannot transport energy away from the core efficiently enough, the stellar material itself will have to move to transport this energy, disrupting hydrostatic equilibrium. We call this disruption convection.

In their derivation, Carroll and Ostlie envision a bubble of gas with its own temperature, pressure, and density in a surrounding gas medium.

Absolute magnitudes and luminosities [Rucinski and Duerbeck, 1997] [Rucinski, 2006]

The classical Roche model allows eclipsing binaries to be separated into morphological types [Terrell, 2001].

2.2.5 Thermal Equilibrium Models

Thermal Equilibrium Models

We know that the two components of a contact binary system have very similar temperatures from observational data. However, observational data also tells us that the two components of contact systems are very rarely equal in mass.

“Up to a third of the energy generated by the primary is transferred to the secondary”[?]

$$\nabla P = -\rho \nabla \Psi \quad (2.10)$$

$$\nabla \rho = \frac{dP(\Psi)}{d\Psi} = \rho(\Psi) \quad (2.11)$$

If we assume a homogenous composition on equipotential surfaces, then all state variables (pressure, density, temperature) are functions of Ψ alone. In order to achieve hydrostatic equilibrium, energy must be exchanged between the two components of the contact binary.

We can construct two model main sequence stars, with masses M_1 and M_2 . Main sequence stars will obey main-sequence scaling relationships, which are well defined laws the describe how stellar radii, density, and temperature vary with stellar mass [Kippenhahn et al., 1990]. The mass - radius relationship is particularly important when constructing contact models.

$$\left(\frac{R}{R_\odot} \right) = \left(\frac{M}{M_\odot} \right)^\alpha \quad (2.12)$$

$$\left(\frac{R_1}{R_2} \right) = \left(\frac{M_1}{M_2} \right)^{0.46} \quad (2.13)$$

Because of the mass - luminosity relationship of main sequence stars, there is a mass ratio - luminosity ratio relationship for the components of contact binaries:

$$\left(\frac{L_1}{L_2} \right) = \left(\frac{M_1}{M_2} \right)^{0.9} \quad (2.14)$$

In order for the binaries to be in contact, their photospheres must touch physically. This allows us to introduce the contact criterion, in which the separation between the centers of the components are equal to the sum of the two radii:

$$a = R_1 + R_2 \quad (2.15)$$

We can relate to the combined masses of the two stars to their periods using the generalized form of Kepler's Third Law:

$$P^2 = \frac{4\pi^2}{G(M_1 + M_2)} a^3 \quad (2.16)$$

Advection is a transport mechanism of a substance, or property (e.g. temperature, density) by a fluid due to the fluid's bulk motion.

[Shu et al., 1976] contact discontinuity model

[Lubow and Shu, 1977]

Gazeas and Stępień [2008] have shown that orbital parameters of contact binary systems obey certain relationships.

$$P = 0.1159 * a^{\frac{3}{2}} M^{\frac{1}{2}} \quad (2.17)$$

Where P is the orbital period in days, $M = M_1 + M_2$ is the total mass of the binary system, and a is the semi major axis of the system in meters.

We can also calculate the orbital angular momentum H_{orb}

$$H_{\text{orb}} = 1.25 \times 10^{52} * M^{\frac{5}{3}} P^{\frac{1}{3}} q (1 + q)^{-2} \quad (2.18)$$

where $q = \frac{M_1}{M_2}$ is the mass ratio of the components.

[Gazeas and Niarchos, 2006]

2.3 Interior Structure

Interior Structure

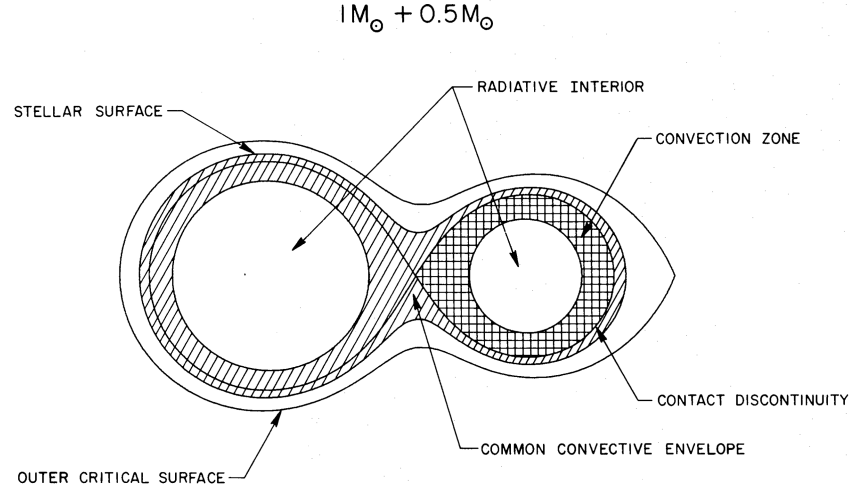


Figure 10: An equatorial cross-section of a $1 M_{\odot} + 0.5 M_{\odot}$ zero-age contact binary of solar composition. The filling factor of this model is $f = 0.41$, and the binary period is $P_d = 0.228$ days. Fig. 2 from Lubow and Shu [1977]

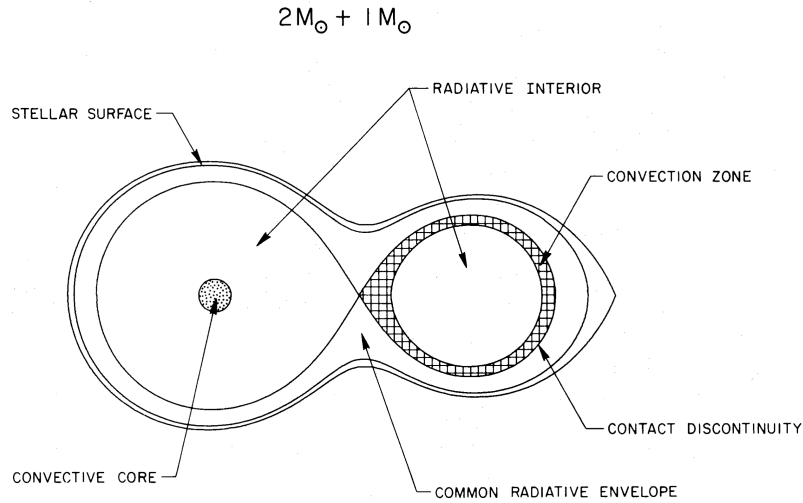


Figure 11: An equatorial cross-section of a $2 M_{\odot} + 1 M_{\odot}$ zero-age contact binary of solar composition. The filling factor of this model is $f = 0.84$, and the binary period is $P_d = 0.314$ days. Fig. 3 from Lubow and Shu [1977]

2.3.1 Common-Envelope Evolution

Common-Envelope Evolution

Common-envelope Evolution, (CEE) [Ivanova et al., 2013]

2.4 Frequency and Density

[Rucinski, 1998a] Studies using OGLE data on the galactic bulge (Baade's Window) indicates that the frequency of contact binaries relative to main sequence stars (or spatial frequency) is approximately $\frac{1}{130} = 0.7\%$, in the absolute magnitude range of $2.5 < M_v < 7.5$. A later study using ASAS data shows that the spatial frequency is 0.2% in the solar neighborhood [Rucinski, 2006] in the absolute magnitude range of $3.5 < M_v < 5.5$.

A catalog of 1022 contact binary systems in ROTSE - 1 data placed the space density of contact binaries at $1.7 \pm 10^{-5} \text{ pc}^{-3}$ [?]

Contact binaries are the most frequently observed type of eclipsing binary star, because their eclipses can be detected at a wide range of orbital inclinations. In recent searches for eclipsing binary stars in survey data [Drake et al., 2014b] contact binary stars comprised 50% of the new variable stars discovered.

Existing catalog of contact binaries in the field [Pribulla et al., 2003]

2.5 Mechanisms of Formation

Formed in Contact. Lucy [1968b] was incorrect in assuming that contact systems exist at Zero Age Main Sequence (ZAMS).

[Yıldız and Doğan, 2013]

[?]

[Li et al., 2007]

Initially Detached, but then inspiral Angular Momentum Loss through stellar winds.

In recent years, evidence has been amassing for the formation via companion pathway. In this pathway, two stars begin in a stable orbit. When a third star is introduced into the system, it steals angular momentum from the first two stars, resulting in a closer orbit.

There is evidence that this companion stays in orbit around the contact binary. A study by Pribulla and Rucinski [2006] has established a lower limit on the number of triple systems. Angular Momentum Loss through tertiary components. [Lohr et al., 2015] In a search of 13,927 eclipsing binaries in the SuperWASP catalog, 24% had period-changes indicating a closely orbiting companion.

In the Kozai-Lidov mechanism , the orbit of two inner bodies is perturbed by a third body orbiting farther out. The equations of motion for the three-body system, a specific angular momentum is conserved:

$$L_z = \sqrt{1 - e^2} \cos i \quad (2.19)$$

Because the quantity L_z is conserved, orbital eccentricity e can be traded for orbital inclination i . So, three body systems with undergo Kozai-Lidov cycles, with a certain period:

$$T_{\text{Kozai}} = 2\pi \frac{\sqrt{GM}}{Gm_2} \frac{a_2^3}{a^{\frac{3}{2}}} (1 - e_2^2)^{\frac{3}{2}} \quad (2.20)$$

2.6 Evolution in the Contact State

Thermal Relaxation Oscillations [Wang, 1994]. May cause orbital period changes observed in Qian [2001].

The structure of contact binaries [Kähler, 2004]

the surface of the contact system does not obey a simple gravity brightening law [Kähler, 2004], [Hilditch et al., 1988].

[Rubenstein, 2001]

Angular momentum and mass evolution. Some of the most recent modeling work indicates that the typical duration of the contact state is 1 to 1.5 Gyr [Gazeas and Stępień, 2008].

masses and angular momenta [Gazeas and Niarchos, 2006] angular momentum loss [Vilhu and Rahunen, 1981]

contact binaries occupy a very narrow range of parameter space [Gazeas, 2009]

Overall evolution [Stepien and Gazeas, 2008], 2016 review of close binary evolution [Tutukov and Cherepashchuk, 2016]

Short period limit [Rucinski, 2007] [Drake et al., 2014a] Lohr et al. [2012] [Rucinski, 1992]

2.7 Evolution out of the Contact State

It is generally accepted that the contact state of binary evolution ends with the inspiral and merger of the two components. The merger event is where the contact system becomes dynamically unstable, and rapidly coalesces into a single, rapidly rotating star.

The tidal interaction between the two components of a contact binary star.

To understand when and why the contact state comes to an end, we must understand the range of conditions over which the contact state is stable.

Merger Tylenda et al. [2011].

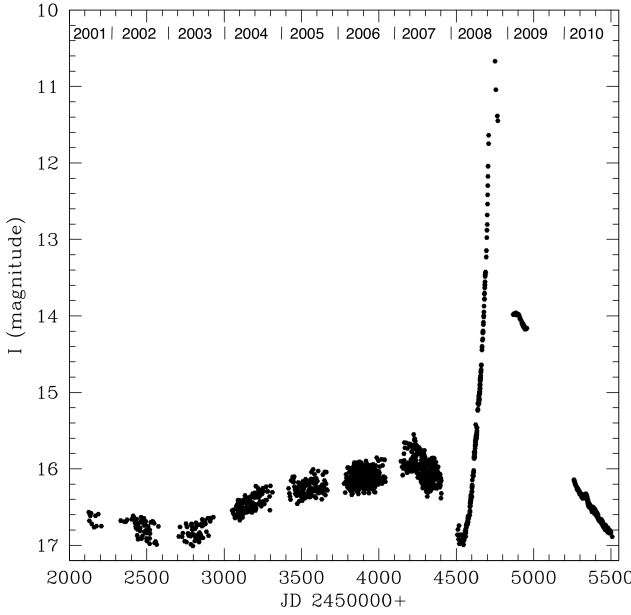


Fig.1. Light curve of V1309 Sco from the OGLE-III and OGLE-IV projects: I magnitude versus time of observations in Julian Dates. Time in years is marked on top of the figure. At maximum the object attained $I \approx 6.8$.

Figure 12: Light curve of V1309 Sco from the OGLE-III and OGLE-IV projects: I magnitude versus time of observations in Julian Dates. Time in years is marked on top of the figure. At maximum the object attained $I \approx 6.8$. Figure 1 from Tylenda et al. [2011]

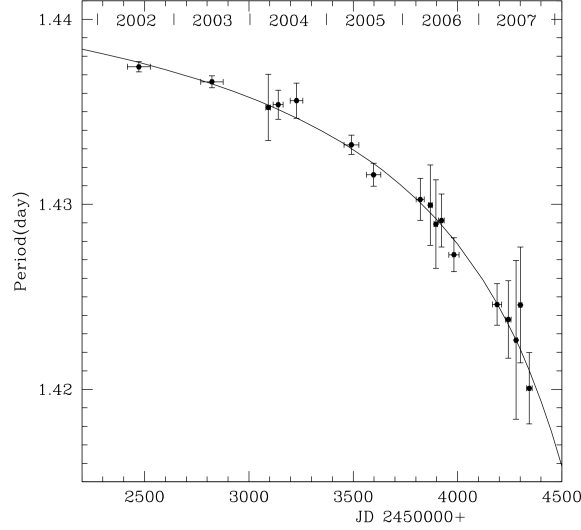


Figure 13: Figure 2 from Tylenda et al. [2011]

The contact binary in the OGLE merger had a period of approximately 1.4 days. Long-period contact binaries [Rucinski, 1998b]

Blue straggler Andronov et al. [2006]

stability of the contact configuration [Rasio, 1995]

One of the ways that a contact binary system can merge is called the Darwin instability.
In a Darwin instability, the ...

In the early 1990s, large numbers of new contact binaries were discovered among blue stragglers, in open and globular clusters

[Kaluzny and Shara, 1988] no discovery in six open clusters.

In the globular cluster M71, four contact binaries discovered by Yan and Mateo [1994], placing a lower limit of 1.3% on the frequency of primordial binaries in M71 with initial orbital periods in the range of 2.5 to 5 days.

Short period eclipsing binaries have been found among blue stragglers in the globular cluster NGC5466 [Mateo et al., 1990].

Review of binaries in globular clusters [Hut et al., 1992]

modern work on six binaries in NGC188 [Chen et al., 2016]

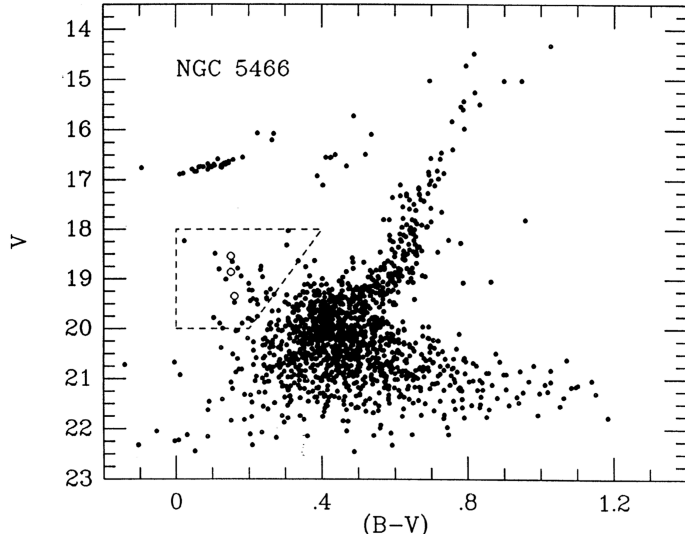


Figure 14: A color-magnitude diagram of globular cluster NGC 5466. The blue stragglers are defined to be all stars located within the region bounded by the dashed lines. The mean V magnitudes and $(B - V)$ colors of the eclipsing binaries discovered by Mateo et al. [1990] are shown as open circles. Figure 1 from Mateo et al. [1990].

2.8 Early-Type Contact Binaries

When astronomers say that a star is “Early-Type”, they mean that it is “early” on the spectral classification sequence (OBAFGKM). O and B stars are more massive, more luminous and hotter than our sun. Early-Type contact binaries deserve a special section due to their extreme mass, luminosity, rarity, and short lifetime. There are only a handful of O and B

Type contact binary systems known. The four best studied systems are TU Muscae [Penny et al., 2008], MY Cam [Lorenzo et al., 2014], UW CMa [Antokhina et al., 2011], V382 Cygni [Popper, 1978].

Over forty have been found in the Small Magellanic Cloud [Hilditch et al., 2005]

Massive contact binaries in M31 [Lee et al., 2014], [Vilardell et al., 2006]

In modern survey data, we can observe individual eclipsing binary systems in nearby galaxies.

2.9 Magnetic Activity

In the solar atmosphere, the movement of plasma in the convective region creates magnetic fields, which in turn affect the motion of that same plasma. Contact binaries are rapidly rotating systems, with orbital periods of 0.2 to 0.8 days (compare this rate with the approximately 30 day solar rotational period), so they have the potential to form much stronger magnetic fields.

There is a lot of evidence that contact binary stars have strong magnetic fields. Astronomers observe changes in their light-curves, indicating that starspots may be appearing and disappearing on their photospheres. Doppler imaging of contact binaries can reveal the shapes and locations of the starspots on the photosphere (Fig. 16)

Because late-type contact binaries have Common Convective Envelopes (or CCEs),

Some authors believe that the existence of the CCE buries the very strong surface magnetic field, which could prevent the production of flares [Qian et al., 2014].

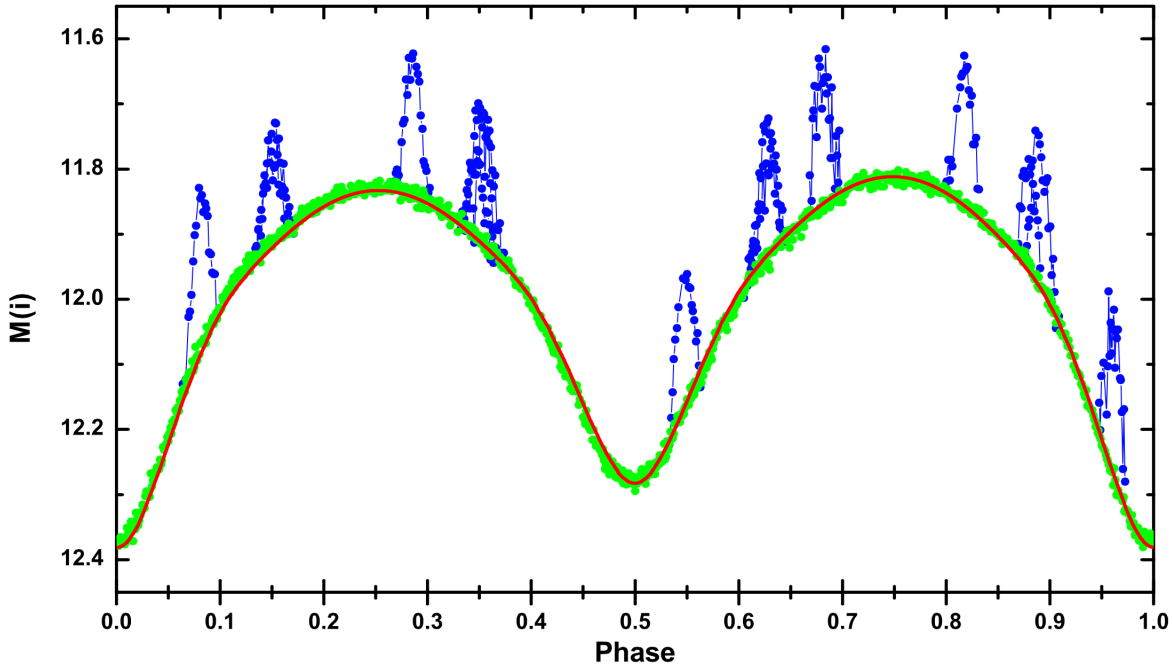


Figure 15: Fig. 15 from Qian et al. [2014]

[Balogh et al., 2015] book review of solar magnetic activity cycles.

The applegate mechanism [Applegate, 1992] [Lanza, 2006]

W UMa as X-ray sources [Stepien et al., 2001]

Observational starspots and magnetic activity cycles. [Borkovits et al., 2005, Shengbang and Qingyao, 2000, Kaszás et al., 1998, Qian et al., 2007, Lee et al., 2004, Yang et al., 2012, Zhang and Zhang, 2004].

It is possible that starspots are responsible for the variation in brightness observed by CRTS. Doppler imaging techniques have confirmed the presence of large starspots on the surface of some contact binaries [Barnes et al., 2004].

Barnes et al. [2004] has used an Echelle spectrograph on the 3.9-meter Anglo-Australian Telescope to perform doppler imaging of the AE Phe system ($P = 0.362$ d), revealing that the photosphere of the system is heavily spotted (Fig. 16).

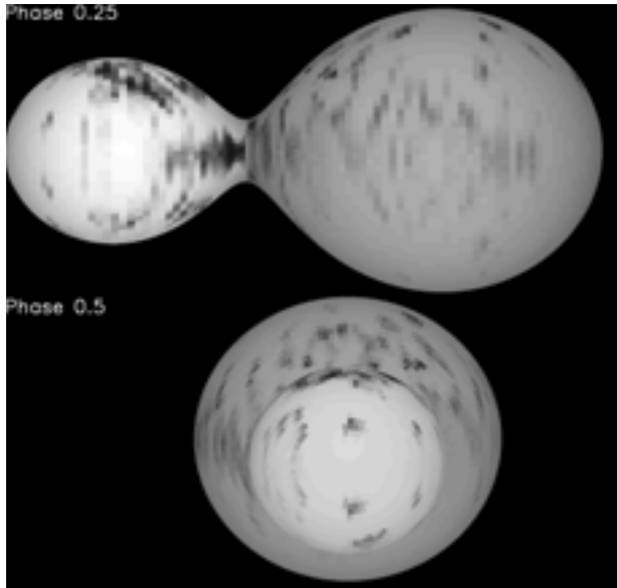


Figure 16: Fig. 5 from Barnes et al. [2004]

The evolution and migration of starspots on contact binaries has been tracked with doppler imaging [Hendry and Mochnacki, 2000] and more recently, in Kepler data [Tran et al., 2013, Balaji et al., 2015]. Starspots are magnetic phenomenon, and so their occurrence is related to the magnetic activity of their host star [Berdyugina, 2005].

2.10 Remaining Questions

3 Observations

Q: What kind of observations can astronomers obtain from contact binary systems?

Astronomy is unique as a science because all the information that can be obtained from an object in the sky comes to us as electromagnetic waves. Perhaps *THE* question in observational astronomy is: “What can we learn from these electromagnetic waves?”. The study of contact binary stars is no different. In this section, we will learn the ways that researchers study electromagnetic waves from contact binary stars.

3.1 Images of Contact Binaries

The oldest type of astronomical information is image data: “What do I see when I look through the telescope?”. To put this question in more formal language: “What is the distribution of the intensity of visible light as a function of position?”. When we look at the moon, for example, we can learn a lot about it: we might see some crater ”over here”, with a given size, shape, color, etc. We might see a dark lunar mare (or “sea”), “over there”, with

another size, shape, color, etc. The moon is what we call a “resolved source”, meaning that features on it are distinguishable: we can separate “over here” from “over there”. In other words, the distance between “over here” and “over there” is larger than the resolution limit of our telescope.

Let’s see if we can reasonably obtain image data from a contact binary:

On a still, clear night at the Las Campanas observatory in Chile, Mike Long reports that the atmospheric resolution limit (or “seeing”) is 0.5 arcseconds. This is the best resolution that can be expected from a telescope on earth: Chile’s Atacama desert is known for some of the best seeing on earth.

$$0.5 \text{ arcseconds} * \frac{1}{3600} \frac{\text{arcseconds}}{\text{degrees}} = 1.4 \times 10^{-4} \text{ degrees} * \frac{\pi}{180} \frac{\text{radians}}{\text{degrees}} = 2.4 \times 10^{-6} \text{ radians} \quad (3.1)$$

In order to distinguish between the two components of a contact binary, the resolution limit of our telescope must be smaller than the distance between the centers of the two components.

For a contact binary star of solar type, this is about one solar radius: $1R_{\odot} = 6.957 \times 10^5 \text{ km}$. Let us place this hypothetical contact binary at the same distance as the nearest star, *Proxima Centauri*, which is 4.243 light years = 1.301 parsecs = $4.014 \times 10^{13} \text{ km}$.

To calculate the angle that a solar type-contact binary at the distance of *Proxima Centauri* would subtend, we will use the small angle approximation:

$$\sin(\theta) \approx \theta, \quad \cos(\theta) \approx 1 - \frac{\theta^2}{2}, \quad \tan(\theta) = \frac{\sin(\theta)}{\cos(\theta)} = \frac{\theta}{1 - \frac{\theta^2}{2}} \Rightarrow \tan(\theta) \approx \theta \quad (3.2)$$

If we set up a right triangle (as in Fig. 17), we see that the tangent of the angle θ is equal to the radius of the sun divided by the distance to *Proxima Centauri*.

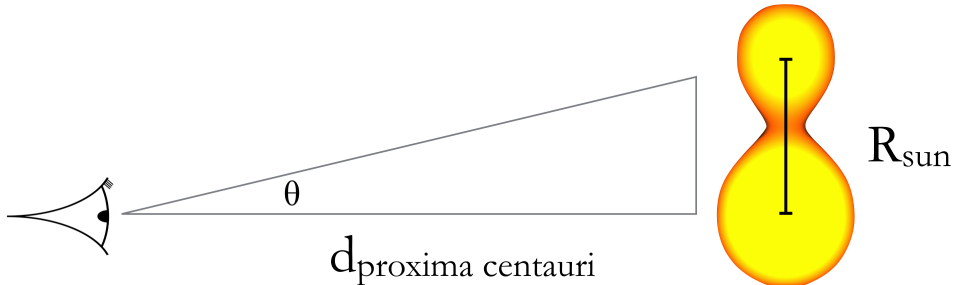


Figure 17: Calculating the angle θ subtended by a solar-type contact binary at the distance of the nearest star.

$$\frac{R_{\text{sun}}}{d_{\text{proxima centauri}}} = \frac{6.957 \times 10^5 \text{ km}}{4.014 \times 10^{13} \text{ km}} = \tan(\theta) \approx \theta = 1.733 \times 10^{-8} \text{ radians} \quad (3.3)$$

When comparing the resolution necessary to distinguish the components of a contact binary to the best resolution possible on earth:

$$\frac{1.733 \times 10^{-8} \text{ radians}}{2.4 \times 10^{-6} \text{ radians}} \approx 0.01 \quad (3.4)$$

To summarize: we would need 100 times the resolving power achievable from the earth to obtain image data from a large contact binary at the distance of the nearest star. In actuality, the situation is worse. 44 Bootis is the nearest contact binary system to earth, at a distance of 13 parsecs (42 light years) it is 10 times further away than *Proxima Centauri* [Eker et al., 2008]. For this reason, we cannot obtain usable image data from contact binaries¹.

3.2 Photometry of Contact Binaries

Q: Why does the flux received from a contact binary vary over time? Q: How was the light-curve used to determine what a contact binary was? Q: How can light-curve data be used to learn about contact binary systems?

In images, contact binaries appear as an unresolved point source. At first glance, it may appear that astronomers are stuck: they cannot “see” the contact binary and so must remain uncertain about its characteristics. However, as Kempf and Müller learned in 1903, the amount of light received from a contact binary varies as a function of time. This function is called the light-curve:

$$f(\text{Time}) = \text{Flux Received at Telescope} \quad (3.5)$$

A light curve is constructed from observations: by repeatedly measuring the brightness of a source over a certain time span, an astronomer can sample the light-curve and approximate its true shape.

Kempf and Müller knew that they could use the light-curve to learn about the shape of the contact binary system. First, they noted that the light-curve was periodic: after a certain amount of time, the trend in flux *exactly repeated* itself. Thus they knew that the process that was responsible for the variation in the flux was cyclical in nature.

¹it is possible to achieve this resolution (as good as 0.0005”) through long-baseline interferometry. Using the CHARA array on Mount Wilson, researchers have constructed a resolved image of the eclipsing binary system β *Lyræ* [Zhao et al., 2008]. However, interferometric imaging is only possible for the brightest stars, so is not useful for contact binaries.

They knew that the period of the light variation in W UMa was very stable (“The error of the period can hardly be more than 0.5s...”). They assumed that a rotational or orbital mechanism was responsible for the light variation. They thought that the presence of a large dark spot on a rapidly rotating single star, which was hypothesized to be “in an advanced stage of cooling”. However, W UMa was a white star, not a cool red star, leading Kempf and Müller to discredit this model. They also considered a single star in the shape of an ellipsoid - a large, however they calculated that this model did not describe the shape of the light-curve very well. In 1903, the eclipsing binary model was already proposed as a mechanism for the light-curves of certain stars (most notably Algol). To construct their model, they looked at existing eclipsing binary light curves and imagined what would happen if they brought the two stars close together. If they brought the two stars close enough together so that the stars were almost touching, there was always variation in the light-curve, just like they observed.

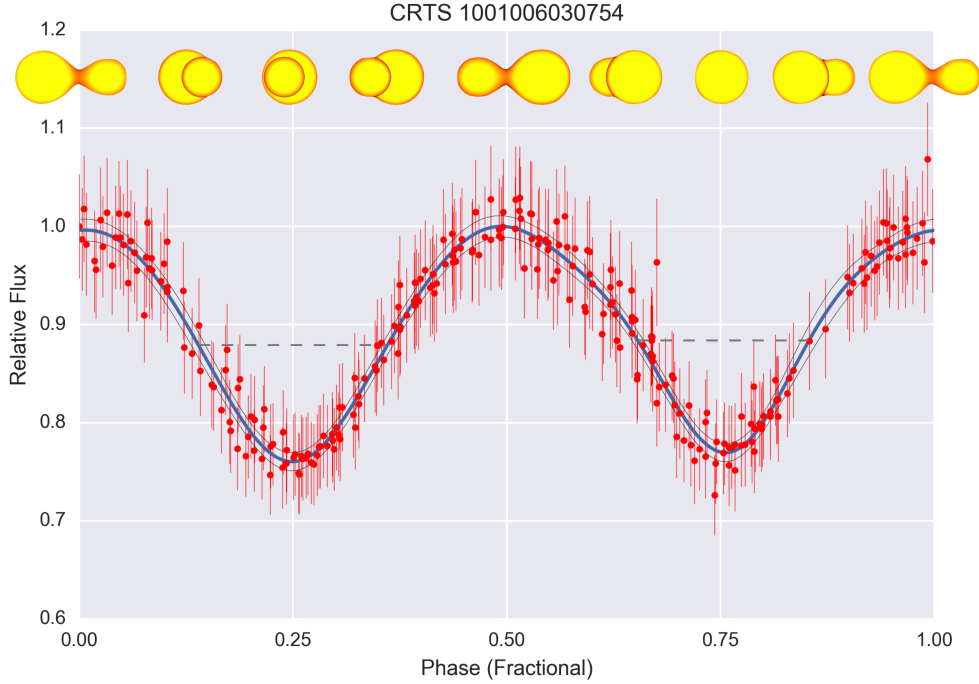


Figure 18: Light-curve is from CRTS data [Drake et al., 2014b]. Illustration of contact binary phase from an animation at: <http://cronodon.com/SpaceTech/BinaryStar.html>

The shape of a contact binary’s light-curve can tell us a lot about it. Indeed, the aim of much of the original work in this thesis is to determine how the shape of the contact binary light-curve correlates with physical parameters. I’ll now go through a few light-curve features

Not all contact binary light-curves look the same, so why is that?

3.2.1 Amplitude

One of the most obvious features of the contact binary light-curve is its Amplitude . The amplitude is how much the brightness of the contact binary varies from its minimum brightness, to its maximum brightness.

3.2.2 Difference Between Eclipse Minima

3.2.3 Difference Between Out-of-Eclipse Maxima

3.2.4 Eclipse Width at Half-Minimum

How much can the shape of the light-curve tell us about the geometry of the contact binary system? When astronomers constructed the first computer models of contact binaries (based on the initial solution in Lucy [1968a]

3.3 Spectra of Contact Binaries

time-series spectra are some of the most complete observations of contact binaries.

Analyzing spectra of contact binaries is challenging. Abundances of elements cannot be determined precisely due to the broadening and blending of spectral lines caused by the fast rotation [Gazeas and Niarchos, 2006].

3.4 X-ray and Ultraviolet Data on Contact Binaries

Earth's atmosphere is opaque to X-ray and ultraviolet (UV) light, but the advent of space-based observatories has made observations of the sky possible in these passbands.

Contact binaries are much brighter than main-sequence stars in the ultraviolet, owing to their strong magnetic fields.

In this section, I describe some of the major sources of modern observations of contact binaries.

Since the late 1990s, photometric surveys that frequently observe large areas of the sky have come online. Through the careful classification of periodic variable sources in survey datasets, larger and larger samples of contact binary systems have been assembled, making studies of contact binaries as a population possible. Previous surveys have compiled variable star catalogs which include many contact binary systems. Examples of such surveys are the All-Sky Automated Survey [ASAS, Pojmanski, 2000], Robotic Optical Transient Search Experiment [ROTSE, Akerlof et al., 2000], Trans-Atlantic Exoplanet Survey [TrES, Devor et al., 2008], Lincoln Near-Earth Asteroid Research program [LINEAR, Palaversa et al., 2013], and Catalina Real-Time Transient Survey [CRTS, Drake et al., 2014b]. Researchers

have also selected pure samples of contact binary systems from large survey data sets for study. Researchers have previously used data from the Optical Gravitational Lensing Experiment [OGLE, Rucinski, 1996], Super Wide Angle Search for Planets [SuperWASP, Norton et al., 2011], and CRTS [Drake et al., 2014a] to construct pure contact binary samples for study. Lee [2015] have used this approach to study a pure sample detached eclipsing binaries from the CRTS variable catalog.



Figure 19: Images of the instruments used in six modern surveys. In the top left, SuperWASP [SuperWASP, Norton et al., 2011], ASAS [ASAS, Pojmanski, 2000], [ROTSE, Akerlof et al., 2000],

3.5 The Kepler Spacecraft

3.6 The Sloan Digital Sky Survey

York et al. [2000]

[Ivezić et al., 2007]

calibrations allow for stellar temperatures to be derived Fukugita et al. [2011]

SEGUE is a program that collects stellar spectra.

3.7 The SuperWASP Survey

follow-up on 1-meter telescopes in South Africa [Koen et al., 2016].

more follow up [Darwish et al., 2016]

3.8 The LINEAR Survey

3.9 The Catalina Surveys

3.10 Other Surveys

OGLE work has determined a criterion for overcontact based on Fourier coefficients [Rucinski, 1997]. [Rucinski, 1993]

Rucinski has used eclipse half-widths and Fourier components to estimate geometrical properties of the system:

[Rucinski, 1973]

the reliability of the mass-ratio determination from light-curve only data [Hambálek and Pribulla, 2013]

ROTSE study using fourier methods [Coker et al., 2013]

phenomenological study [Andronov, 2012]

3.11 Future Surveys



Figure 20

4 Analysis Techniques

Q: How do astronomers use their observations to learn about the physical characteristics of contact binary systems?

Observational tests of theories of contact binaries Lucy and Wilson [1979]

4.1 Physical Light-Curve Modeling

In §3.2, we learned about how contact binary light-curves contain information about the physical nature of the system. Since the majority of data on contact binaries is in the form of photometric light-curve measurements, there has been much effort spent on refining the process of light-curve analysis.

In this section, we will learn how physical models can be fit to observational light-curves.

The Wilson-Devinney Code

Fully automated approaches [Prsa et al., 2009] [Prsa et al., 2008]

recent advances in modeling code [Prša et al., 2013]

employing neural networks to find true binary parameters [Zeraatgari et al., 2015]

4.2 O-C Analysis

O-C Analysis is short for “observed minus computed”, referring to the fact that a measurement is the observed time of minimum light as compared to the computed time of minimum light.

1. A full light curve is obtained for the system in question.
2. Based on this light curve, the period is calculated, and an ephemeris is computed, listing all of the future times of minimum light.
3. Then, light curves are obtained at future epochs. The time of minimum light are compared to previous times of minimum light. The difference ($O - C$) is plotted as a function of epoch.

On an O-C diagram, a linear change in period appears as a parabola.

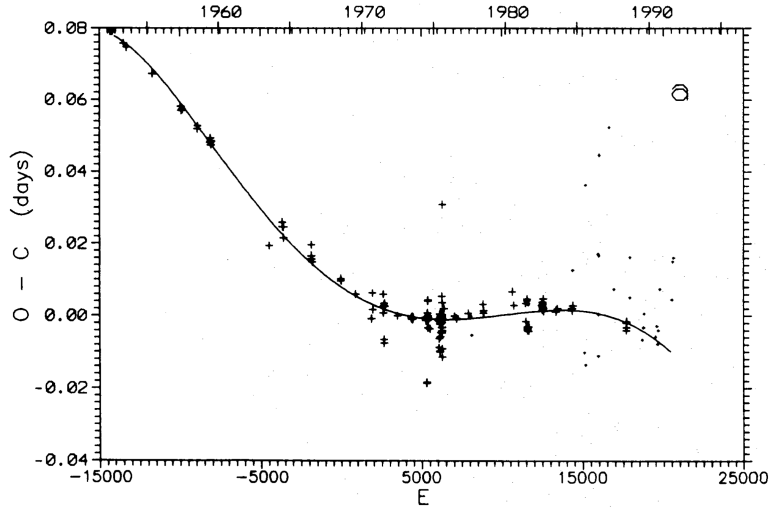


Figure 21: The O - C diagram of V566 Oph, fit by a least squares polynomial. Fig. 4a from Kalimeris et al. [1994]

On orbital period change [Kalimeris et al., 1994]

The orbital period of a contact binary can change for a variety of reasons, but an observed period change always implies underlying geometrical and structural changes.

In contact systems, orbital period changes can generally be divided into (1) short-term variations, which happen on decadal (10 year) timescales, and (2) long-term variations, which happen on a thermal timescale.

The long-term variations are caused by

- 1) Angular momentum loss due to magnetic braking.
- 2) mass loss through the L_2 point
- 3) chemical evolution of the primary.

The short-term variations are caused by

- 1) The orbit of a third body
- 2) Redistribution of the angular momentum due to magnetic activity.
- 3) Is O-C Analysis stable against the appearance and disappearance of starspots and photometric noise? [Kalimeris et al., 2002]

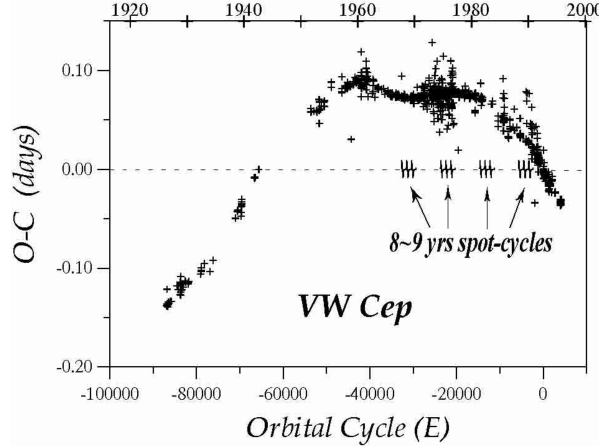


Figure 22: Fig. 7 from Kalimeris et al. [2002]

automated approach with SuperWASP [Lohr et al., 2015]

In data from surveys, the data may be too sparse to estimate times of minimum light from multiple epochs within the survey. A Lomb-Scargle (or LS) [Scargle, 1982] [Horne and Baliunas, 1986]

$$|\delta P| = (0.01728 \text{ s}) \times \left(\frac{N_0}{100}\right)^{-\frac{1}{2}} \times \left(\frac{T_{eff}}{5\text{yr}}\right)^{-1} \times \left(\frac{A/\sigma_N}{10}\right)^{-1} \times \left(\frac{P}{0.2\text{d}}\right)^2 \quad (4.1)$$

Qian [2001] has observed orbital period changes which indicate TRO.

4.3 Doppler Imaging

5 Pause

Data from large All-Sky surveys is very different in nature compared with data taken on a single night with a single telescope. Working with all-sky surveys presents huge advantages to working with traditional light-curve data, but it also has major drawbacks.

In “traditional” variable star observing, an observer slews the telescope to the target at the beginning of the night, and then takes a continuous sequence of images (from which she will make photometric measurements) at regularly spaced time intervals, until the star has rotated one full period, or until morning twilight. The observer can only look at one target at once, but the selected target is observed many times in one night.

In All-Sky surveys, the observing mode is different. All throughout the night, the telescope pans to a field, taking a few images, and then rapidly moving on to the next field. A given source might only be observed one or two times in a given night. The survey operates night after night, and after several years, it has amassed hundreds of observations of any point on the sky.

When we look in a survey database for photometric measurements of a known contact binary we often see data that looks like the data in Figure 23.

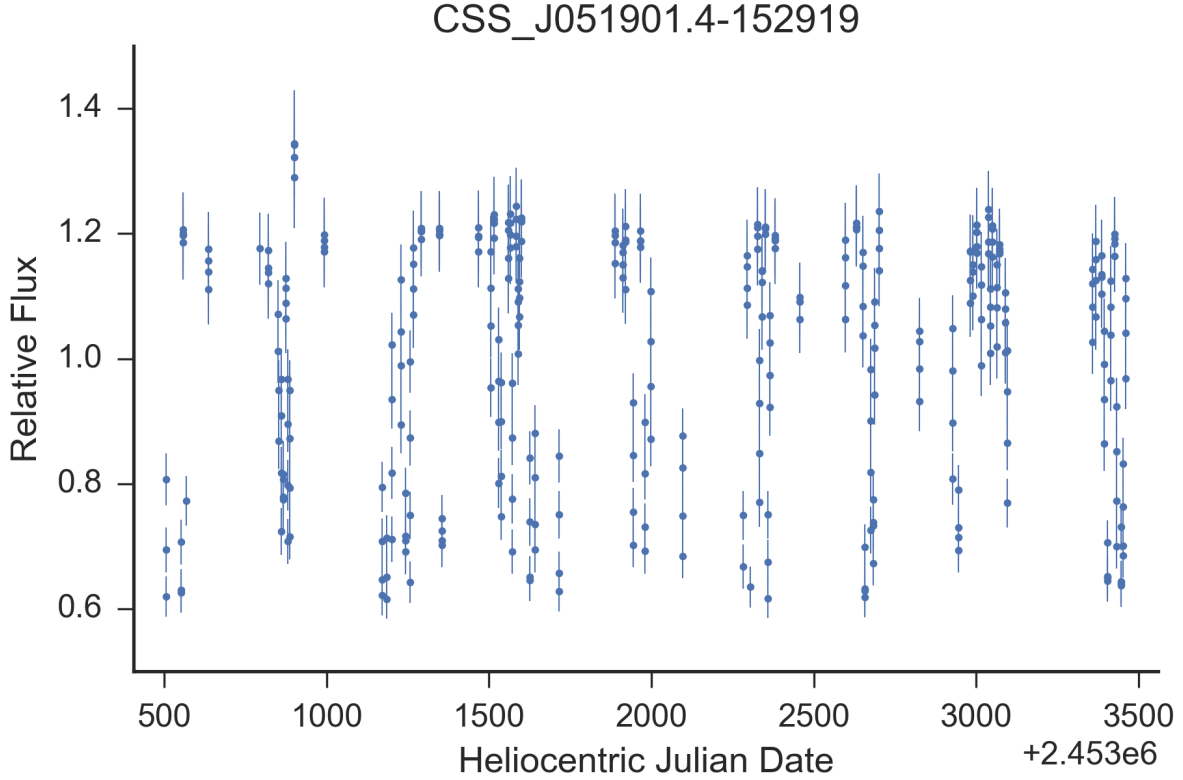


Figure 23: Observations of a contact binary, as returned by CRTS. The x-axis is the time of observation (in days), and the y-axis is the relative flux of the observation. Vertical bars about each point denote the uncertainty in the relative flux measurement. Note that the observed flux varies significantly from observation to observation, but we cannot see the periodic nature of the variability with our eyes

We know that the data in Figure 23 is not data from a source with constant brightness. Look at the size of the error bar on each point. The error bar on each point is much smaller than the scatter in the distribution. We would call this source a variable source.

Hidden in this data is an underlying periodic function - the light-curve caused by the rotation of the contact binary. The period is hidden in this data, we just need to find it.

The data that we have here is a *time-series*: a number of measurements of the flux of a source at many different times. The problem of finding a period in time-series data is usually handled with a *Fourier Transform*.

In the Fourier Transform,

The CRTS telescope does not return to this source at regular times.

The algorithm that is most widely used to find periods in unevenly sampled time-series Scargle [1982]

We calculate the phase of each observation, by dividing by the period found in the signal.

$$\theta = \frac{(\text{Time \% Period})}{\text{Period}} \quad (5.1)$$

where (%) is the “modulo” (or remainder operator)

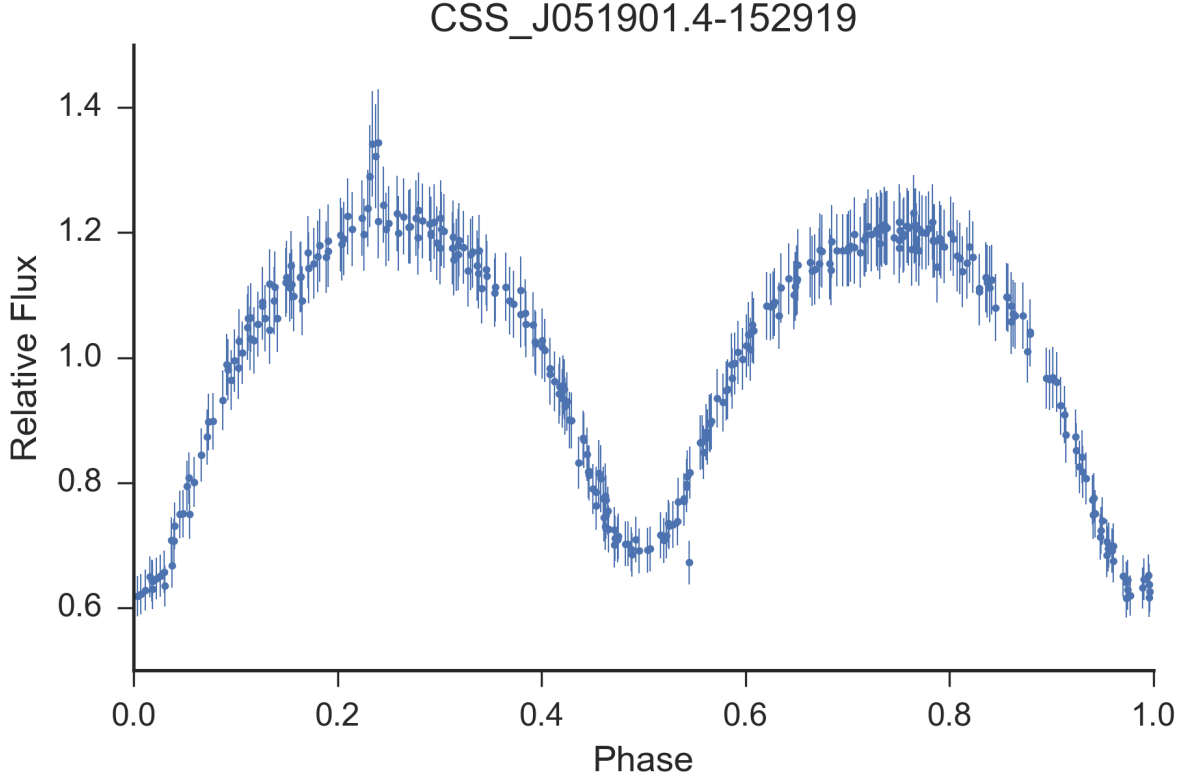


Figure 24: Observations of a contact binary by CRTS, folded by the period as detected by the lomb-scargle algorithm.

In Figure 24, we see survey data of a contact binary, after it has been folded by the orbital period. We see a coherent light-curve with a beautiful shape.

6 Light-curve Morphology

§ begins the “original research” part of the thesis. In this section we aim to learn how contact binary light-curves vary as a function of photospheric temperature. We have access to over

9,000 white-light light-curves from the CRTS survey and multicolor photometry from the SDSS survey. This is all the data we will need to begin our study.

6.1 Our Observations

6.2 Light-curve Features

In order to understand how the light-curves change as a function of temperature, we must first figure out a way to describe a light-curve in a way that makes sense, both to humans and computers. In data science, this problem is called “feature selection” . Let’s consider what our light curve data actually is: a set of measurements of the flux of a contact binary. These measurements are taken at a certain time (t), have a certain value, in our case a measurement of flux (f), and this measured value has an associated error (e). From CRTS, we obtain lots of these measurements. Our light curve looks like this:

Table 1: Format of Raw Data from CRTS

time (t)	flux (f)	error (e)
number	number	number
number	number	number
...

In §5, we were able to construct a coherent light-curve out of survey data taken at random times by folding the data by the orbital period. Just as before, we can input out data into a Lomb-Scargle , or similar period-finding algorithm, find the best period p and fold the observations by that period. This returns us a new version of the light-curve:

Table 2: Format of Phase-folded Data from CRTS

phase (θ)	flux (f)	error (e)
number	number	number
number	number	number
...

In the eight years between 2005 and 2013, CRTS observes a given source roughly 350 times. In other words, it reports about 350 phases (θ), 350 fluxes (f), and 350 errors (e) on those fluxes. So, the raw data comes to us as $\approx 350 \times 3 = 1050$ individual numbers.

These numbers are perfectly valid descriptors of the light-curve, but they are not easily understandable, neither by a human nor a computer.

Thankfully, we can introduce some assumptions that will make the task of succinctly describing our light-curves easier. First, we assume that our light-curve is a *continuous function*. This means that there are not jumps or breaks in the true variation of light. The light-curve has a value at every point in phase, and is differentiable at every point in phase. Second, we assume that *the light-curve is periodic*: that the pattern of light variation will exactly repeat itself after some amount of time. In §7, we learn that this is not exactly true for contact binaries when we observe them over many years. But for now, this assumption will serve us well.

Now, armed with our two new assumptions and light-curve data, we can construct a light-curve function. There are many ways to construct a continuous, periodic function from a set of data.

1. Polynomial Fit.

$$f(\theta) = a_0 + a_1\theta + a_1\theta^2 + a_2\theta^3 + \dots (0 \leq p < 1)$$

$$f(\theta) = \sum_{i=0}^n a_i \theta^i (0 \leq \theta < 1) \quad (6.1)$$

2. Polynomial - Spline Fit.

$$f(p) = \dots \quad (6.2)$$

[Gettel et al., 2006] a spline fit is employed. [Akerlof et al., 1994] explanation of spline fit.

3. Fourier (Harmonic) Fit.

$$f(p) =$$

$$f(p) = \sum_{i=0}^n a_i \cos(2\pi i p) \quad (6.3)$$

There are many other forms that can be used to represent a continuous periodic function - but these are the most obvious choices. Each has advantages and disadvantages. For

example, if the light-curve has large derivatives at some points in the phase (it has “sharp turns”), a polynomial spline fit may be the best choice.

We have elected to use the harmonic fit, because it has a history of use in the description contact binary light-curves. It is easy to implement and can fit the data accurately, provided that there are not sharp turns.

By choosing a fitting function, we have turned our raw data from CRTS (which was 1000 numbers) into a continuous, periodic function which we can use to derive other, physically meaningful features.

Recall (as in Eqn. 3.5)

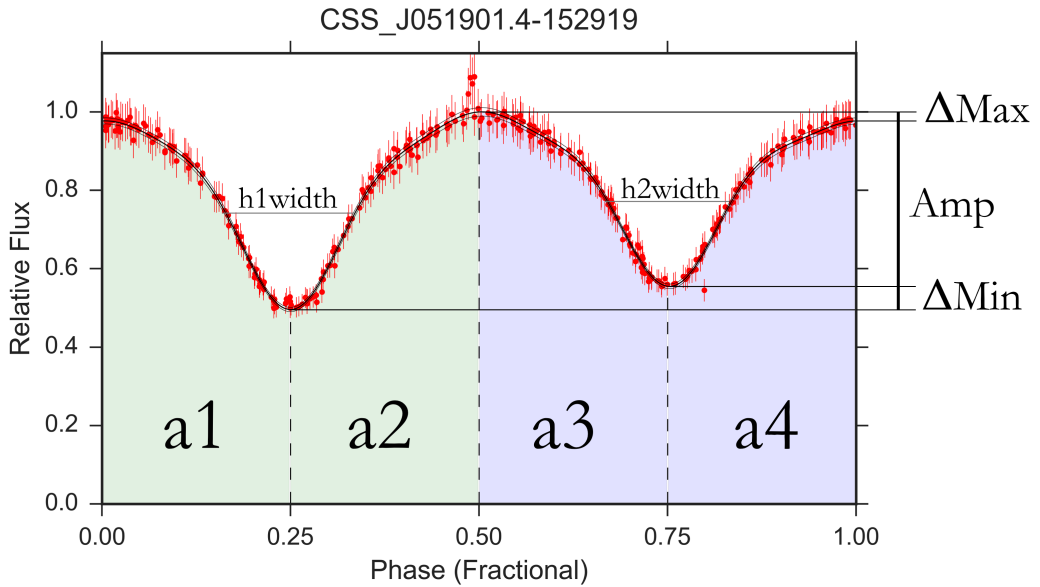


Figure 25: A graphical description of the light-curve features that we derive for contact binaries in our sample.

For each light-curve, we have derived the following geometrical features:

Areas (a_1, a_2, a_3, a_4). The features have units of energy, being products of phase (which is time), and flux (which is rate at which energy is received by the telescope.)

Flux Differences (Amp, Δ_{Min} , Δ_{Max}). These features have units of flux, because they are differences of fluxes. Eclipse Width and Half Minimum. ($h_1\text{width}$, $h_2\text{width}$). These features have units of time, because they are differences of phases.

In the following mathematical descriptions of the light-curve features, we will compute the light-curve on a grid of at least 500 points spaced evenly in phase. The relative flux computed from the harmonic fit at a point i is denoted F_i . This is the y -coordinate on the light-curve graph. The phase of the point i is denoted by P_i . This is the x -coordinate on the light-curve graph.

The area features were computed as Riemann sums on a fixed, evenly spaced, grid of discrete phases:

$$\begin{aligned}
a1 &= \frac{\sum_i F_i}{\sum_i 1} (0 < P_i \leq 0.25) \\
a2 &= \frac{\sum_i F_i}{\sum_i 1} (0.25 < P_i \leq 0.50) \\
a3 &= \frac{\sum_i F_i}{\sum_i 1} (0.50 < P_i \leq 0.75) \\
a4 &= \frac{\sum_i F_i}{\sum_i 1} (0.75 < P_i \leq 1.00)
\end{aligned} \tag{6.4}$$

The following light-curve features have units of flux. The light-curve amplitude (Amp) is the total range of the flux variation, ranging from a maximum at 1.0 (by the definition of our flux, see Eqn.??) to the lowest value of the light-curve, $F_{\min 1}$. The flux difference between eclipse minima (ΔMin) is the difference between the flux at the second local minimum in the light curve $F_{\min 2}$, and the flux at the lowest value of the light-curve, $F_{\min 1}$. The flux difference between out-of-eclipse maxima

$$\begin{aligned}
\text{Amp} &= 1.0 - F_{\min 1} \\
\Delta\text{Min} &= F_{\min 2} - F_{\min 1} \\
\Delta\text{Max} &= 1.0 - F_{\max}
\end{aligned} \tag{6.5}$$

We also compute two intermediate flux features that will help us calculate the eclipse full-width at half-minimum.

$$\begin{aligned}
F_{h1} &= 0.5 + \frac{F_{\min 1}}{2} \\
F_{h2} &= 0.5 + \frac{F_{\min 2}}{2}
\end{aligned} \tag{6.6}$$

The following light-curve features have units of time. P_{h1} and P_{h2} are the closest points in phase.

$$h1width = P_{h1} - P_{h1}$$

$$h2width = P_{h2} - P_{h2}$$

(6.7)

O'Connell [1951]

7 Luminosity Variation on a Decadal Timescale

In our study, we aim to learn how the luminosity of contact binary systems vary on decadal timescales. In §?? we talked about the light-curve as if it was one single function. In actuality, the shape of contact binary light-curves change over time (Eqn. ??).

$$f(\text{Phase, Time}) = \text{Flux Received at Telescope} \quad (7.1)$$

We can detect light-curve changes with a survey that observes the same set of contact binaries over a timespan of several years (like CRTS).

In order to detect changes in the contact binary light-curve in CRTS data, we will re-use much of the machinery that we have developed in §??.

[Bradstreet and Guinan, 1988]

8 Detection of Flares

In our study, we aim to learn about the flaring frequency of contact binaries and to determine if flare characteristics vary as a function of photospheric temperature.

READ Walkowicz et al. 2011 and Shibayama et al. 2013.

Contact binaries are known X-ray sources [Chen et al., 2006]. Flare have been observed in X-ray bands using ROSAT [McGale et al., 1996]. EXOSAT has been used to observe a flare in X-ray and Microwave data on VW Cephei ($P = 0.28$ days, $T_1, T_2 = 5500\text{K}, 5000\text{K}$) [Vilhu et al., 1988]. Extreme UV observations have identified coronal characteristics [Brickhouse and Dupree, 1998]. Long time series observations of single m-dwarfs [Lacy et al., 1976]

During a continuous monitoring campaign in the winters of 2008 and 2010, Qian et al. [2014] observed a contact binary system CSTAR 038663 ($P = 0.27$ days, $T_1, T_2 = 4616\text{K}, 4352\text{K}$) for a total of 4167 hours (174 days) in the SDSS i band using the CSTAR telescope array in the Antarctic. In this time, Qian et al. [2014] discovered 15 i band flares, revealing a flare rate of 0.0036 flares per hour. These 15 flares had durations ranging from 0.006 to

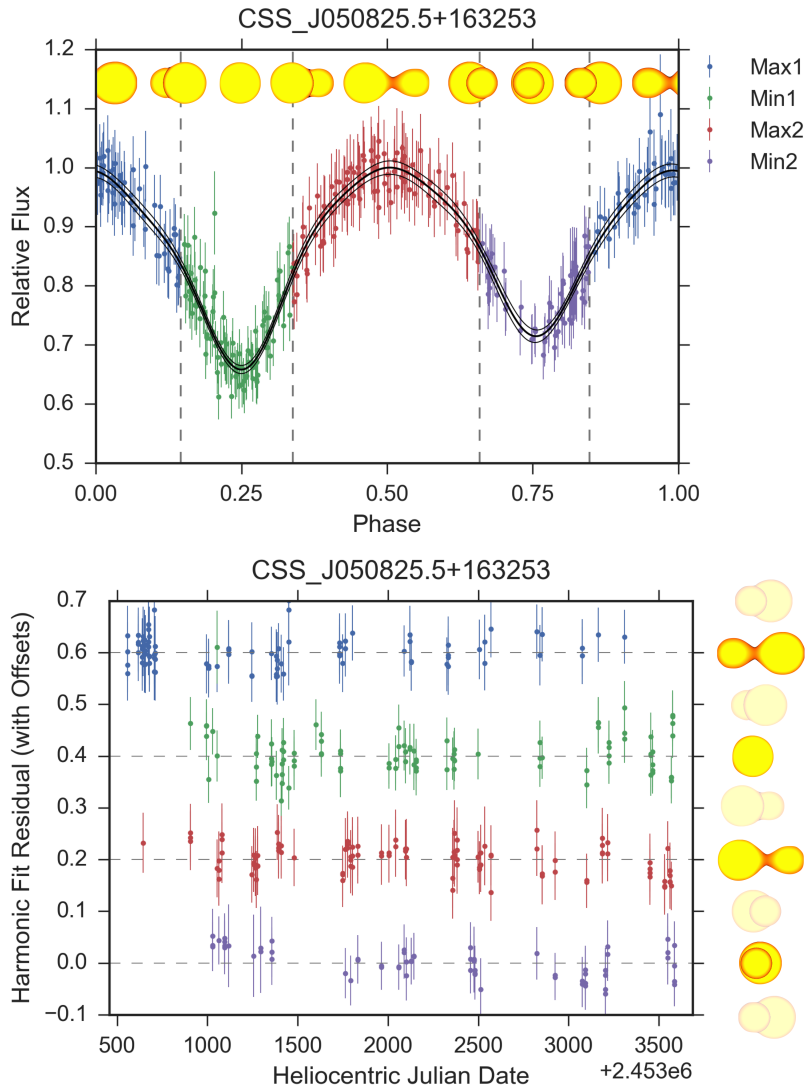


Figure 26: The light-curve of a contact binary as observed by CRTS. In the top panel, we see that the light-curve is normalized in flux such that the maximum value of the harmonic fit (in black) is 1.0. We see that the light-curve has been divided into four distinct regions by phase. In the bottom panel, we see the harmonic fit residuals as a function of observation time. Observations from each one of the four bins have been separated. The light-curve of this contact binary does not change over the eight-year observation timespan, the residuals are centered around 0 for observations in each phase bin. The orbital period of this binary is 0.323716 days. The variability amplitude of this object binary is 0.57.

0.014 days (9 to 20 minutes), and amplitudes ranging from 0.14 - 0.27 magnitudes above the quiescent magnitude.

In 1049 close binaries observed by Kepler, Gao et al. [2016] have identified 234 “flare binaries”, on which a total of 6818 flares were detected. Kepler’s continuous monitoring capability and precise photometry make it extremely well suited to the detection of white-light flares [Walkowicz et al., 2011]. While CRTS does not match Kepler’s observing cadence, photometric precision, or ability to observe a given target continuously, it observes 33,000 square degrees a much larger area of the sky than Kepler does (100 square degrees) [Drake et al., 2009, Basri et al., 2005].

M-dwarfs have previously been searched for flares in Sloan Digital Sky Survey Stripe 82 data [Kowalski et al., 2009]. Our study will be similar to that of Kowalski et al. [2009], because we are also using survey observations of large regions of sky, as opposed to the continuous monitoring studies. Hilton et al. [2010] have discovered flares in the time resolved SDSS spectroscopic sample, using a Flare Line Index based on H α and H β line strength.

In CRTS data, we monitor 9851 contact binaries. We aim to verify the relationships described in Gao et al. [2016], and focus on the contact binary subclass. We aim to place better constraints on the flare rate as a function of both orbital period and photospheric temperature. The dataset constitutes the equivalent of 40.6 years of monitoring continuous monitoring at an average cadence of one 30 second observation per 9 minutes.

9 Conclusion

Index

- L_2 , 35
- β Lyrae, 29
- Algol, 30
- Early-Type, 24
- equations of stellar structure, 12
- feature selection, 39
- Fourier Transform, 37
- Hertzprung-Russell Diagram, 12
- Inner Jacobi Equipotential, 15
- Kempf, Paul Friedrich Ferdinand, 7
- Kozai-Lidov mechanism, 21
- light-curve, 29
- Müller, Karl Hermann Gustav, 7
- Potsdam Observatory, 7
- time-series, 37
- Zöllner's photometer, 7

References

- C Akerlof, S Amrose, R Balsano, J Bloch, D Casperson, S Fletcher, G Gisler, J Hills, R Kehoe, B Lee, et al. Rotse all-sky surveys for variable stars. i. test fields. *The Astronomical Journal*, 119(4):1901, 2000.
- Carl Akerlof, C Alcock, R Allsman, T Axelrod, DP Bennett, KH Cook, K Freeman, K Griest, S Marshall, H-S Park, et al. Application of cubic splines to the spectral analysis of unequally spaced data. *The Astrophysical Journal*, 436:787–794, 1994.
- Ivan L Andronov. Phenomenological modeling of the light curves of algol-type eclipsing binary stars. *Astrophysics*, 55(4):536–550, 2012.
- N Andronov, MH Pinsonneault, and DM Terndrup. Mergers of close primordial binaries. *The Astrophysical Journal*, 646(2):1160, 2006.
- EA Antokhina, M Srinivasa Rao, and M Parthasarathy. Light curve analysis of hipparcos data for the massive o-type eclipsing binary uw cma. *New Astronomy*, 16(3):177–182, 2011.
- James H Applegate. A mechanism for orbital period modulation in close binaries. *The Astrophysical Journal*, 385:621–629, 1992.
- Bhaskaran Balaji, Bryce Croll, Alan M Levine, and Saul Rappaport. Tracking the stellar longitudes of starspots in short-period kepler binaries. *Monthly Notices of the Royal Astronomical Society*, 448(1):429–444, 2015.
- André Balogh, Hugh Hudson, Kristóf Petrovay, and Rudolf Steiger. *The Solar Activity Cycle: Physical Causes and Consequences*, volume 53. Springer, 2015.
- JR Barnes, TA Lister, RW Hilditch, and A Collier Cameron. High-resolution doppler images of the spotted contact binary ae phe. *Monthly Notices of the Royal Astronomical Society*, 348(4):1321–1331, 2004.
- Gibor Basri, William J Borucki, and David Koch. The kepler mission: A wide-field transit search for terrestrial planets. *New Astronomy Reviews*, 49(7):478–485, 2005.
- Svetlana V Berdyugina. Starspots: a key to the stellar dynamo. *Living Rev. Solar Phys.*, 2:8, 2005.
- Marvin Bolt, Thomas Hockey, JoAnn Palmeri, Virginia Trimble, Thomas R Williams, Katherine Bracher, Richard Jarrell, Jordan D Marché, and F Jamil Ragep. *Biographical encyclopedia of astronomers*. Springer Science & Business Media, 2007.

T Borkovits, MM Elkhateeb, Sz Csizmadia, J Nuspl, IB Biró, T Hegedüs, and R Csorvási. Indirect evidence for short period magnetic cycles in w uma stars-period analysis of five overcontact systems. *Astronomy & Astrophysics*, 441(3):1087–1097, 2005.

David H Bradstreet and Edward F Guinan. Mapping of surface activity on the w uma-type system vw cephei. 1988.

NS Brickhouse and AK Dupree. Extreme ultraviolet explorer observations of the w ursae majoris contact binary 44i bootis: Coronal structure and variability. *The Astrophysical Journal*, 502(2):918, 1998.

Bradley W Carroll and Dale A Ostlie. *An introduction to modern astrophysics and cosmology*, volume 1. 2006.

WP Chen, Kaushar Sanchawala, and MC Chiu. W ursae majoris contact binary variables as x-ray sources. *The Astronomical Journal*, 131(2):990, 2006.

Xiaodian Chen, Licai Deng, Richard de Grijs, Xiaobin Zhang, Yu Xin, Kun Wang, Changqing Luo, Zhengzhou Yan, Jianfeng Tian, Jinjiang Sun, et al. Physical parameter study of eight w ursae majoris-type contact binaries in ngc 188. *arXiv preprint arXiv:1607.06152*, 2016.

D Coker, S Özdemir, C Yeşilyaprak, SK Yerli, N Aksaker, and BB Güçsav. A study on w ursae majoris-type systems recognised by the rotse-iiid experiment. *Publications of the Astronomical Society of Australia*, 30:e013, 2013.

MS Darwish, MM Elkhateeb, MI Nouh, SM Saad, MA Hamdy, MM Beheary, K Gadallah, and I Zaid. Orbital solution and evolutionary state for the eclipsing binary 1swasp j080150. 03+ 471433.8. *arXiv preprint arXiv:1606.07510*, 2016.

Jonathan Devor, David Charbonneau, Francis T O'Donovan, Georgi Mandushev, and Guillermo Torres. Identification, classifications, and absolute properties of 773 eclipsing binaries found in the trans-atlantic exoplanet survey. *The Astronomical Journal*, 135(3):850, 2008.

AJ Drake, SG Djorgovski, A Mahabal, E Beshore, S Larson, MJ Graham, R Williams, E Christensen, M Catelan, A Boattini, et al. First results from the catalina real-time transient survey. *The Astrophysical Journal*, 696(1):870, 2009.

AJ Drake, SG Djorgovski, D García-Álvarez, MJ Graham, M Catelan, AA Mahabal, C Donalek, JL Prieto, G Torrealba, S Abraham, et al. Ultra-short period binaries from the catalina surveys. *The Astrophysical Journal*, 790(2):157, 2014a.

- AJ Drake, MJ Graham, SG Djorgovski, M Catelan, AA Mahabal, G Torrealba, D García-Álvarez, C Donalek, JL Prieto, R Williams, et al. The catalina surveys periodic variable star catalog. *The Astrophysical Journal Supplement Series*, 213(1):9, 2014b.
- Z Eker, S Bilir, E Yaz, O Demircan, and M Helvacı. New absolute magnitude calibrations for w ursa majoris type binaries. *arXiv preprint arXiv:0807.4989*, 2008.
- Masataka Fukugita, Naoki Yasuda, Mamoru Doi, James E Gunn, and Donald G York. Characterization of sloan digital sky survey stellar photometry. *The Astronomical Journal*, 141(2):47, 2011.
- Qing Gao, Yu Xin, Ji-Feng Liu, Xiao-Bin Zhang, and Shuang Gao. White-light flares on close binaries observed with kepler. *arXiv preprint arXiv:1602.07972*, 2016.
- K Gazeas and K Stępień. Angular momentum and mass evolution of contact binaries. *Monthly Notices of the Royal Astronomical Society*, 390(4):1577–1586, 2008.
- KD Gazeas. Physical parameters of contact binaries through 2-d and 3-d correlation diagrams. *Communications in Asteroseismology*, 159:129–130, 2009.
- KD Gazeas and PG Niarchos. Masses and angular momenta of contact binary stars. *Monthly Notices of the Royal Astronomical Society: Letters*, 370(1):L29–L32, 2006.
- Sara J Gettel, Michael T Geske, and Tim A McKay. A catalog of 1022 bright contact binary stars. *The Astronomical Journal*, 131(1):621, 2006.
- L Hambálek and T Pribulla. The reliability of mass-ratio determination from light curves of contact binary stars. *Contributions of the Astronomical Observatory Skalnate Pleso*, 43: 27–46, 2013.
- Paul D Hendry and Stefan W Mochnacki. Doppler imaging of vw cephei: distribution and evolution of starspots on a contact binary. *The Astrophysical Journal*, 531(1):467, 2000.
- RW Hilditch, DJ King, and TM McFarlane. The evolutionary state of contact and near-contact binary stars. *Monthly Notices of the Royal Astronomical Society*, 231(2):341–352, 1988.
- RW Hilditch, ID Howarth, and TJ Harries. Forty eclipsing binaries in the small magellanic cloud: fundamental parameters and cloud distance. *Monthly Notices of the Royal Astronomical Society*, 357(1):304–324, 2005.

Eric J Hilton, Andrew A West, Suzanne L Hawley, and Adam F Kowalski. M dwarf flares from time-resolved Sloan Digital Sky Survey spectra. *The Astronomical Journal*, 140(5):1402, 2010.

James H Horne and Sallie L Baliunas. A prescription for period analysis of unevenly sampled time series. *The Astrophysical Journal*, 302:757–763, 1986.

Piet Hut, Steve McMillan, Jeremy Goodman, Mario Mateo, ES Phinney, Carlton Pryor, Harvey B Richer, Frank Verbunt, and Martin Weinberg. Binaries in globular clusters. *Publications of the Astronomical Society of the Pacific*, pages 981–1034, 1992.

N Ivanova, S Justham, X Chen, O De Marco, CL Fryer, E Gaburov, H Ge, E Glebbeek, Z Han, X-D Li, et al. Common envelope evolution: where we stand and how we can move forward. *The Astronomy and Astrophysics Review*, 21(1):1–73, 2013.

Željko Ivezić, J Allyn Smith, Gajus Miknaitis, Huan Lin, Douglas Tucker, Robert H Lupton, James E Gunn, Gillian R Knapp, Michael A Strauss, Branimir Sesar, et al. Sloan digital sky survey standard star catalog for stripe 82: The dawn of industrial 1% optical photometry. *The Astronomical Journal*, 134(3):973, 2007.

H Kähler. The structure of contact binaries. *Astronomy & Astrophysics*, 414(1):317–333, 2004.

A Kalimeris, H Rovithis-Livaniou, and P Rovithis. On the orbital period changes in contact binaries. *Astronomy and Astrophysics*, 282:775–786, 1994.

A Kalimeris, H Rovithis-Livaniou, and P Rovithis. Starspots and photometric noise on observed minus calculated (o–c) diagrams. *Astronomy & Astrophysics*, 387(3):969–976, 2002.

Josef Kallrath and Eugene F Milone. *Eclipsing binary stars: modeling and analysis*. Springer, 2009.

Janusz Kaluzny and Michael M Shara. A ccd survey for contact binaries in six open clusters. *The Astronomical Journal*, 95:785–793, 1988.

G Kaszás, J Vinkó, K Szatmáry, T Hegedus, J Gal, LL Kiss, and T Borkovits. Period variation and surface activity of the contact binary vw cephei. *Astronomy and Astrophysics*, 331:231–243, 1998.

Rudolf Kippenhahn, Alfred Weigert, and Achim Weiss. *Stellar structure and evolution*, volume 44. Springer, 1990.

C Koen, T Koen, and RO Gray. Multi-filter light curves of 29 very short period candidate contact binaries. *The Astronomical Journal*, 151(6):168, 2016.

Zdenek Kopal. Close binary systems. *The International Astrophysics Series, London: Chapman & Hall*, 1959, 1959.

Adam F Kowalski, Suzanne L Hawley, Eric J Hilton, Andrew C Becker, Andrew A West, John J Bochanski, and Branimir Sesar. M dwarfs in Sloan Digital Sky Survey stripe 82: Photometric light curves and flare rate analysis based on observations obtained with the Apache Point Observatory 3.5 m telescope, which is owned and operated by the astrophysical research consortium. *The Astronomical Journal*, 138(2):633, 2009.

Kevin Krisciunas. A brief history of astronomical brightness determination methods at optical wavelengths. *arXiv preprint astro-ph/0106313*, 2001.

Gerard P Kuiper. On the interpretation of beta Lyrae and other close binaries. *The Astrophysical Journal*, 93:133, 1941.

CLAUD H Lacy, Th J Moffett, and DAVID S Evans. Uv Ceti stars-statistical analysis of observational data. *The Astrophysical Journal Supplement Series*, 30:85–96, 1976.

Antonino F Lanza. Internal stellar rotation and orbital period modulation in close binary systems. *Monthly Notices of the Royal Astronomical Society*, 369(4):1773–1779, 2006.

C-H Lee, J Koppenhoefer, S Seitz, R Bender, A Riffeser, M Kodric, U Hopp, J Snigula, C Gössl, R-P Kudritzki, et al. Properties of M31. v. 298 eclipsing binaries from Pan-STARRS. *The Astrophysical Journal*, 797(1):22, 2014.

Chien-Hsiu Lee. Properties of eclipsing binaries from all-sky surveys–ii. detached eclipsing binaries in Catalina Sky Surveys. *Monthly Notices of the Royal Astronomical Society*, 454(3):2946–2953, 2015.

Jae Woo Lee, Chun-Hwey Kim, Wonyong Han, Ho-Il Kim, and Robert H Koch. Period and light variations for the cool, overcontact binary BX Pegasi. *Monthly Notices of the Royal Astronomical Society*, 352(3):1041–1055, 2004.

Lifang Li, Fenghui Zhang, Zhanwen Han, and Dengkai Jiang. Formation and evolution of w Ursae Majoris contact binaries. *The Astrophysical Journal*, 662(1):596, 2007.

ME Lohr, AJ Norton, UC Kolb, DR Anderson, Francesca Faedi, and Richard G West. Period decrease in three SuperWASP eclipsing binary candidates near the short-period limit. *Astronomy & Astrophysics*, 542:A124, 2012.

ME Lohr, AJ Norton, SG Payne, RG West, and PJ Wheatley. Orbital period changes and the higher-order multiplicity fraction amongst superwasp eclipsing binaries. *arXiv preprint arXiv:1505.00941*, 2015.

J Lorenzo, I Negueruela, AKF Val Baker, Miriam García, Sergio Simón-Díaz, P Pastor, and M Méndez Majuelos. My camelopardalis, a very massive merger progenitor. *Astronomy & Astrophysics*, 572:A110, 2014.

SH Lubow and FH Shu. On the structure of contact binaries. ii-zero-age models. *The Astrophysical Journal*, 216:517–525, 1977.

LB Lucy. The light curves of w ursae majoris stars. *The Astrophysical Journal*, 153:877, 1968a.

LB Lucy. The structure of contact binaries. *The Astrophysical Journal*, 151:1123, 1968b.

LB Lucy and RE Wilson. Observational tests of theories of contact binaries. *The Astrophysical Journal*, 231:502–513, 1979.

Mario Mateo, Hugh C Harris, James Nemec, and Edward W Olszewski. Blue stragglers as remnants of stellar mergers—the discovery of short-period eclipsing binaries in the globular cluster ngc 5466. *The Astronomical Journal*, 100:469–484, 1990.

PA McGale, JP Pye, and ST Hodgkin. Rosat pspc x-ray spectral survey of w uma systems. *Monthly Notices of the Royal Astronomical Society*, 280:627–637, 1996.

SW Mochnacki. Accurate integrations of the roche model. *The Astrophysical Journal Supplement Series*, 55:551–561, 1984.

SW Mochnacki and NA Doughty. A model for the totally eclipsing w ursae majoris system aw uma. *Monthly Notices of the Royal Astronomical Society*, 156(1):51–65, 1972.

G Muller and P Kempf. A new variable star unusually short period. *The Astrophysical Journal*, 17:201–211, 1903.

Andrew J Norton, SG Payne, T Evans, Richard G West, Peter J Wheatley, DR Anderson, SCC Barros, OW Butters, A Collier Cameron, Damian Joseph Christian, et al. Short period eclipsing binary candidates identified using superwasp. *Astronomy & Astrophysics*, 528:A90, 2011.

DJK O’Connell. The so-called periastron effect in close eclipsing binaries; new variable stars (fifth list). *Publications of the Riverview College Observatory*, 2:85–100, 1951.

Lovro Palaversa, Željko Ivezić, Laurent Eyer, Domagoj Ruždjak, Davor Sudar, Mario Galin, Andrea Kroflin, Martina Mesarić, Petra Munk, Dijana Vrbanec, et al. Exploring the variable sky with linear. iii. classification of periodic light curves. *The Astronomical Journal*, 146(4):101, 2013.

Laura R Penny, Cynthia Ouzts, and Douglas R Gies. Tomographic separation of composite spectra. xi. the physical properties of the massive close binary hd 100213 (tu muscae). *The Astrophysical Journal*, 681(1):554, 2008.

G Pojmanski. The all sky automated survey. catalog of about 3800 variable stars. *Acta Astronomica*, 50:177–190, 2000.

DM Popper. Masses of hot main-sequence stars. *The Astrophysical Journal*, 220:L11–L14, 1978.

T Pribulla, JM Kreiner, and J Tremko. Catalogue of the field contact binary stars. *Contributions of the Astronomical Observatory Skalnate Pleso*, 33:38–70, 2003.

Theodor Pribulla and Slavek M Rucinski. Contact binaries with additional components. i. the extant data. *The Astronomical Journal*, 131(6):2986, 2006.

James Edward Pringle and Richard Alan Wade. Interacting binary stars. 1985.

A Prsa, EF Guinan, EJ Devinney, SG Engle, M DeGeorge, GP McCook, PA Maurone, J Pepper, DJ James, DH Bradstreet, et al. Fully automated approaches to analyze large-scale astronomy survey data. *arXiv preprint arXiv:0904.0739*, 2009.

A Prša, P Degroote, K Conroy, S Bloemen, K Hambleton, J Giamarco, and H Pablo. Physics of eclipsing binaries: Motivation for the new-age modeling suite. *EAS Publications Series*, 64:259–268, 2013.

Andrej Prsa, EF Guinan, EJ Devinney, M DeGeorge, DH Bradstreet, JM Giamarco, CR Alcock, and SG Engle. Artificial intelligence approach to the determination of physical properties of eclipsing binaries. i. the ebai project. *The Astrophysical Journal*, 687(1):542, 2008.

S-B Qian, J-Z Yuan, B Soonthornthum, L-Y Zhu, J-J He, and Y-G Yang. Ad cancri: A shallow contact solar-type eclipsing binary and evidence for a dwarf third component and a 16 year magnetic cycle. *The Astrophysical Journal*, 671(1):811, 2007.

S-B Qian, J-J Wang, L-Y Zhu, B Snoonthornthum, L-Z Wang, EG Zhao, X Zhou, W-P Liao, and N-P Liu. Optical flares and a long-lived dark spot on a cool shallow contact binary. *The Astrophysical Journal Supplement Series*, 212(1):4, 2014.

Shengbang Qian. Orbital period changes of contact binary systems: direct evidence for thermal relaxation oscillation theory. *Monthly Notices of the Royal Astronomical Society*, 328(3):914–924, 2001.

Frederic A Rasio. The minimum mass ratio of w ursae majoris binaries. *arXiv preprint astro-ph/9502028*, 1995.

Eric P Rubenstein. The effect of stellar evolution on population ii contact binaries in the period-color relation. i. equal-mass, marginal contact systems. *The Astronomical Journal*, 121(6):3219, 2001.

Slavek M Rucinski. Eclipsing binaries in the ogle variable star catalog. ii. light curves of the w uma-type systems in baade’s window. *arXiv preprint astro-ph/9611158*, 1996.

Slavek M Rucinski. Eclipsing binaries in the ogle variable star catalog. iw uma-type systems as distance and population tracers in baade’s window. *The Astronomical Journal*, 113: 407, 1997.

Slavek M Rucinski. Contact binaries of the galactic disk: Comparison of the baade’s window and open cluster samples. *The Astronomical Journal*, 116(6):2998, 1998a.

Slavek M Rucinski. Eclipsing binaries in the ogle variable star catalog. iii. long-period contact systems. *The Astronomical Journal*, 115(3):1135, 1998b.

Slavek M Rucinski. Luminosity function of contact binaries based on the all sky automated survey (asas). *Monthly Notices of the Royal Astronomical Society*, 368(3):1319–1322, 2006.

Slavek M Rucinski. The short-period end of the contact binary period distribution based on the all-sky automated survey. *Monthly Notices of the Royal Astronomical Society*, 382(1): 393–396, 2007.

Slavek M Rucinski and Hilmar W Duerbeck. Absolute magnitude calibration for the w uma-type contact binary stars. In *Hipparcos-Venice’97*, volume 402, pages 457–460, 1997.

SM Rucinski. The w uma-type systems as contact binaries. i. two methods of geometrical elements determination. degree of contact. *Acta Astronomica*, 23:79, 1973.

SM Rucinski. Can full convection explain the observed short-period limit of the w uma-type binaries? *The Astronomical Journal*, 103:960–966, 1992.

SM Rucinski. A simple description of light curves of w uma systems. *Publications of the Astronomical Society of the Pacific*, pages 1433–1440, 1993.

Jeffrey D Scargle. Studies in astronomical time series analysis. ii-statistical aspects of spectral analysis of unevenly spaced data. *The Astrophysical Journal*, 263:835–853, 1982.

Qian Shengbang and Liu Qingyao. A possible connection between the variation of light curve and thechange of the orbital period in the contact binary ck bootis. *Astrophysics and Space Science*, 271(4):331–339, 2000.

FH Shu, SH Lubow, and L Anderson. On the structure of contact binaries. i-the contact discontinuity. *The Astrophysical Journal*, 209:536–546, 1976.

Marc Van Der Sluys. Roche potential, 2006. URL <http://hemel.waarnemen.com/Informatie/Sterren/hoofdstuk6.html#h6.2>.

Klaus Staubermann. The trouble with the instrument: Zöllner’s photometer. *Journal for the History of Astronomy*, 31:323, 2000.

K Stepień and K Gazeas. Evolutionary scenario for w uma-type stars. *Proceedings of the International Astronomical Union*, 4(S252):427–428, 2008.

K Stepień, JHMM Schmitt, and W Voges. Rosat all-sky survey of w ursae majoris stars and the problem of supersaturation. *Astronomy & Astrophysics*, 370(1):157–169, 2001.

Dirk Terrell. Eclipsing binary stars: Past, present, and future. *Journal of the American Association of Variable Star Observers (JAAVSO)*, 30:1, 2001.

K Tran, A Levine, S Rappaport, T Borkovits, Sz Csizmadia, and B Kalomeni. The anti-correlated nature of the primary and secondary eclipse timing variations for the kepler contact binaries. *The Astrophysical Journal*, 774(1):81, 2013.

AV Tutukov and AM Cherepashchuk. The evolution of close binary stars. *Astronomy Reports*, 60(5):461–476, 2016.

R Tylenda, M Hajduk, T Kamiński, A Udalski, I Soszyński, MK Szymański, M Kubiak, G Pietrzyński, R Poleski, K Ulaczyk, et al. V1309 scorpii: merger of a contact binary. *Astronomy & Astrophysics*, 528:A114, 2011.

F Vilardell, I Ribas, and C Jordi. Eclipsing binaries suitable for distance determination in the andromeda galaxy. *Astronomy & Astrophysics*, 459(1):321–331, 2006.

Osmi Vilhu, Jean-Pierre Caillault, and John Heise. Simultaneous exosat and vla observations of the contact binaries vw cephei and xy leonis-quiescent emission and a flare on vw cephei. *The Astrophysical Journal*, 330:922–927, 1988.

Osrai Vilhu and Timo Rahunen. Contact binary evolution and angular momentum loss. In *Fundamental problems in the theory of stellar evolution*, volume 93, page 181, 1981.

Lucianne M Walkowicz, Gibor Basri, Natalie Batalha, Ronald L Gilliland, Jon Jenkins, William J Borucki, David Koch, Doug Caldwell, Andrea K Dupree, David W Latham, et al. White-light flares on cool stars in the kepler quarter 1 data. *The Astronomical Journal*, 141(2):50, 2011.

J-M Wang. The thermal relaxation oscillation states of contact binaries. *The Astrophysical Journal*, 434:277–282, 1994.

RF Webbink. Contact binaries. In *3D Stellar Evolution*, volume 293, page 76, 2003.

RE Wilson. Binary star morphology and the name overcontact. *Information Bulletin on Variable Stars*, 2001.

Lin Yan and Mario Mateo. Primordial main sequence binary stars in the globular cluster m71. *The Astronomical Journal*, 108:1810–1827, 1994.

Y-G Yang, S-B Qian, and B Soonthornthum. Deep, low-mass ratio overcontact binary systems. xii. ck bootis with possible cyclic magnetic activity and additional companion. *The Astronomical Journal*, 143(5):122, 2012.

Mutlu Yıldız and T Doğan. On the origin of w uma type contact binaries—a new method for computation of initial masses. *Monthly Notices of the Royal Astronomical Society*, page stt028, 2013.

Donald G York, J Adelman, John E Anderson Jr, Scott F Anderson, James Annis, Neta A Bahcall, JA Bakken, Robert Barkhouse, Steven Bastian, Eileen Berman, et al. The sloan digital sky survey: Technical summary. *The Astronomical Journal*, 120(3):1579, 2000.

FZ Zeraatgari, A Abedi, M Farshad, M Ebadian, N Riazi, J Nedoroščík, M Vaňko, T Pribulla, D Kjurkchieva, V Popov, et al. Neural network analysis of w uma eclipsing binaries. *Contrib. Astron. Obs. Skalnaté Pleso*, 45:5–16, 2015.

XB Zhang and RX Zhang. Long-term photometric study of the w uma binary star v523 cas. *Monthly Notices of the Royal Astronomical Society*, 347(1):307–315, 2004.

M Zhao, D Gies, JD Monnier, N Thureau, E Pedretti, F Baron, A Merand, T Ten Brummelaar, H McAlister, ST Ridgway, et al. First resolved images of the eclipsing and interacting binary β lyrae. *The Astrophysical Journal Letters*, 684(2):L95, 2008.